GRANULARITY CHARACTERISTICS OF AN ELECTRON EXPOSED PHOTOGRAPHIC EMULSION

by

Harry Nash Hodges, Jr.

A Thesis Submitted to the Faculty of the

COMMITTEE ON OPTICAL SCIENCES (GRADUATE)

In Partial Fulfillment of the Requirements
For the Degree of

MASTER OF SCIENCE

In the Graduate College

THE UNIVERSITY OF ARIZONA

1 9 7 5

STATEMENT BY AUTHOR

This thesis has been submitted in partial fulfillment of requirements for an advanced degree at The University of Arizona and is deposited in the University Library to be made available to borrowers under rules of the Library.

Brief quotations from this thesis are allowable without special permission, provided that accurate acknowledgment of source is made. Requests for permission for extended quotation from or reproduction of this manuscript in whole or in part may be granted by the head of the major department or the Dean of the Graduate College when in his judgment the proposed use of the material is in the interests of scholarship. In all other instances, however, permission must be obtained from the author.

SIGNED: Harry M Hodges

APPROVAL BY THESIS DIRECTOR

This thesis has been approved on the date shown below:

P N Slater

PHILIP N. SLATER
Professor of Optical Sciences

17 December 1975
Date

ACKNOWLEDGMENTS

I must first acknowledge the assistance of the Eastman Kodak Company for their donation of the SO-219 film and their permission to present the data sheets; then Dr. Lee Kelly of The University of Arizona who assisted me in the use of his electron microscope; Dr. Peter Bartels of The University for the use of his microdensitometer; my advisor, Dr. James Eyer, for his advice and encouragement. I thank especially Dr. Phil Slater for his long patience and persistence. Finally, I must acknowledge the United States Air Force for financial assistance.

TABLE OF CONTENTS

LIST OF ILLUSTRATIONS

LIST OF ILLUSTRATIONS--Continued

LIST OF TABLES

ABSTRACT

A special direct electron recording film, Eastman Kodak SO-219, has been tested experimentally by exposure to light and 20, 15, and 10 KV electrons from a defocused electron microscope beam. The D-Log E curves were obtained and the electron exposed emulsions showed a non-linear D-E curve beyond a D = 0.75, and showed reciprocity failure between 30 and 800 pa/sq cm intensity levels for 15 and 20 KEV exposures. Granularity ($\sigma(D)$) was determined up to a D = 3.0 using two square apertures of 6.25 and 1.57 μm. The photon $\text{Log}_{10}(D)$-Log D curve was of the form anticipated with $\sigma(D)$ increasing slowly with D to about D = 1.0 where $\sigma(D)$ began to increase rapidly. Electron exposures showed a faster increase of $\sigma(D)$ to a maximum value depending on the exposing energy. After this maximum, the $\sigma(D)$ began to decrease as D increased. The experimentally determined relationship between $\sigma(D)$ and D was not in agreement with previously published theoretical data. The disagreement is attributed to the choice of the grain-to-electron ratio used in the theoretical data. The DQE of this emulsion is less than 0.3 for all tested voltages. The number of distinguishable density levels was determined to be 15 for photon exposures and 11 for 15 KV electrons at ±5 $\sigma(D)$ levels. A brief summary of other research in electron exposure is given.

CHAPTER 1

INTRODUCTION

Presently, there are many operational and proposed systems employing silver halide emulsions to record information using electrons for the exposing energy. One of the considerations involved in the design of such a system is the noise, or granularity, of the recording material. This paper discusses the granularity of a fine grained, electron recording film, Eastman Kodak's SO-219.

This paper is organized into three major sections. The first briefly summarizes electron recording systems, the differences between electron and photon exposures, and the granularity for each type of exposure. The second section defines the experimental conditions concerning exposure, processing, densitometry, and data reduction. The last section discusses the experimental results.

Summary of Present Systems Using Electron Beam Recording

The earliest demonstration of electron beam recording (EBR), as opposed to electron distribution recording, on a silver halide film was that of Tarnowski and Evans in 1962. They constructed an experimental 16mm recorder to obtain engineering data on resolution

capabilities, especially at low acceleration voltages. Exposing knife edges on a specially prepared emulsion, they obtained modulation transfer factors (MTF) better than 0.35 at 400 lp/mm. Other tests evaluated MTF as a function of potential, emulsion type, and writing beam spot size. Their paper demonstrated in particular the speed and convenience of silver halide recording over thermo-plastic.

It was not until 1966, however, that a practical EBR system evolved (Reed, 1966). Using a standard emulsion, it recorded television images at a low acceleration potential. Its unique feature was a dual vacuum system; the electron gun being held at a higher vacuum than the film. This reduced cathode wear and allowed faster film changing. Since the recorder was designed primarily for standard 525 line television, its noise properties and resolution capabilities were not fully exploited. This system is available commercially from the 3M Company (3M Company, 1968).

As this EBR television recorder developed, many of its advantages over direct phosphor recording became obvious (Dubbe, 1966). A particular gain in EBR is the decrease of noise from a phosphor. Additional gains are realized in the elimination of the TV interlace and picture splice problems. While complications are added due to the required vacuum system, overall, the electron system has considerably more quality.

The commercial exploitation of EBR in television recording continues with the CBS Electronic Video Recorder (EVR). The CBS system employs 8mm film and requires a special reader. The recorder writes 3 tracks of information (2 rows of images, 1 row for optical synchronization), and leaves 2 tracks for magnetic sound. Recording at 60 frames per second, a 750 ft cartridge (7 inch diameter by 1/2 inch thick) will run 24 minutes; the reader scans one row of images and reverses to scan the second row. Each image frame is 2.5 by 3.5mm (1/2 the standard 8mm frame) and the entire TV frame is recorded. Even at the small frame size, the capabilities of the film have not been used; the required resolution is less than 200 lines per mm, while the film is capable of more than 400 (Mannheim, 1969).

A different commercial application is 3M Company's computer output EBR system (3M Company, 1969). It writes characters on a dry process, heat developed, 16mm silver film. Writing at magnetic tape drive rates, it produces direct microfilm copies of computer output. The recorder features a 97 character set, including 11 Greek letters, which can be printed horizontally or vertically (bold, medium, or light faced) at rates of 1200 characters/sec. Quality is stated to be "comparable to current microfilm standards."

A military application of EBR which uses the high sensitivity of silver halide film is the facsimile machine

built for the Air Force Avionics Laboratory. Since silver materials have sensitivities which exceed all other recording materials by a factor of 100 to 1000 (Nitka, 1963), high writing rates and large bandwidths are obtainable. The Air Force facsimile machine reads and records 4.5 inch continuous strip photography at a 20 MHz bandwidth with 100 lp/mm resolution (Herbert, 1969).

Although none of the systems discussed utilized fully the capabilities of EBR, such systems are likely to be developed when, for example, updating of the IBM film chip memory at the Lawrence Radiation Laboratory is required (Thornley, Brown, and Speth, 1964). As the hardware evolves there should be corresponding advances in the capabilities of the silver halide emulsions used. Through this new hardware and film it should then be possible to record without adding additional noise, signals containing coded video information transmitted, say, from satellites. Using the long response scale of silver materials exposed by electrons and coding the scale into distinguishable density levels as discussed by Eyer (1962), a recording could be made containing virtually all of the useful information in the original scene, provided the receptor granularity is small enough. Determining this granularity is the aim of this study.

CHAPTER 2

RESPONSE OF PHOTOGRAPHIC MATERIALS TO ELECTRON EXPOSURE

There are several pertinent characteristics of photographic materials. They are: the density vs log exposure (D-Log E) curve, the reciprocity curve, the spectral sensitivity curve, the modulation transfer function (MTF), and the Wiener (noise power) spectrum or granularity. Because these characteristics are very different for electron exposure, they will be described briefly. For more detailed information see Mees and James (1966, Chapters 10, 23).

The Macroscopic Input-Output Relation

The first striking difference between electron and photon exposure is the macroscopic response, output density as a function of input exposure (or log exposure). The primary reason for this difference is that one electron is usually sufficient to cause at least one silver halide grain to become developable, whereas at least two photons (and usually more) are required for photon exposures. In addition, the electron's high ionizing ability means that often one electron can make many grains developable.

Assuming that at most only two electron hits are required to make a grain developable, Hamilton and Marchant (1967) derived the macro response curve for electrons. This function is given as:

$$D = Dmax \{1-[1+sM]e^{-M(s+d)}\} \quad (1)$$

and

$$Dmax = (0.434)\ NA/a, \quad (2)$$

where D is the optical density; M is the average number of electrons striking a cell area a; of spread function size; N is the average number of grains in area a; A is the mean projected area of a grain; and d,s are the probabilities that a grain will require one or two electrons, respectively, to become developable. Note that M, the exposure, is the product of the current density, the area a, and the exposure time.

Further assuming that the factor (Ms) is nearly zero and the factor (Md) is small (thus D is small), then the following approximation is valid:

$$1-e^{-Md} \simeq Md. \quad (3)$$

Then we obtain

$$D = Dmax\ Md. \quad (4)$$

This linear relation between density and exposure has been verified by many investigators, especially at low densities. The length of the linear portion depends mainly on the value of Dmax and the probability s; at high

densities the majority of the remaining grains require more than one electron hit and the s probability becomes significant. Digby, Firth, and Hercock (1953) found that for some emulsions the linear part extended to a density of one-fourth of the maximum density. Other investigators since Digby et al. have found a linear relation to hold especially when specular (rather than diffuse) densities are recorded (Mees and James, 1966, Chapter 10). This dependence on densitometer characteristics was investigated by Vernier (1969); he found nearly perfect linearity under the proper de sitometric conditions.

The action of light on a photographic emulsion is not as simple. Each grain size class has associated with it a probability distribution that a given number of absorbed photons will produce developability. This number typically varies between 10 and 25 (Mees and James, 1966, pp. 76-81), and may be much higher. Because of this the relation between density and exposure is complicated. Webb (1939) reports for multiple hits:

$$D = D_{max} \{1-e^{-EA}(\sum_{n=0}^{r-1} (EA)^n/n!)\} \qquad (5)$$

where E is exposure in photons per unit area, A is grain area, and r is the number of absorbed quanta required to produce developability. This function holds for a single grain size class; the total response is represented by a sum of functions, each for a particular grain size class.

As a consequence different emulsions have different D-Log E curve shapes when exposed to light.

Hamilton and Marchant (1967) point out that emulsions exposed by electrons have identical D-Log E curve shapes, except near Dmax where there are grains which absorb energy but are already in a developable state. Because of this general similarity of shape, an emulsion response curve can be very nearly described by a speed value and a maximum density. The speed value generally used is the slope of the D-E curve as the exposure approaches zero (Valentine, 1966; Zeitler and Hayes, 1965). This speed value is a linear function of the number of developable grains produced per electron and the mean projected area per grain. Unfortunately, both speed and Dmax are affected by the incident electron energy.

Spectral Sensitivity and Reciprocity Failure

The photographic response as a function of incident energy is specified by the spectral sensitivity curve. Generally determined at a constant density, its shape is given by Figure 1. This curve shape has been experimentally verified for both electrons and X-rays (Mees and James, 1966, p. 184; Digby et al., 1953; Takagi, Kitamura, and Morimoto, 1961; Baker, Ramberg, and Hillier, 1942; Van Horn, 1951).

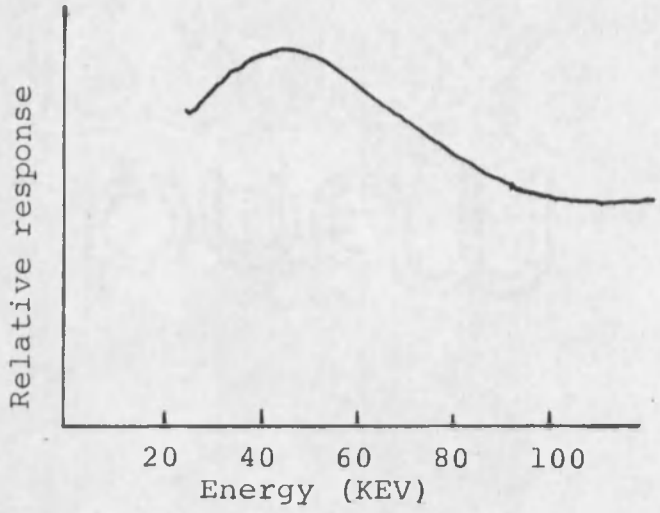

Figure 1. Typical spectral sensitivity.

As stated previously, emulsion speed is a function of the number of developable grains per electron and the mean projected area per grain. Both quantities depend on the electron range. As the electron energy increases, the range increases, depending on the emulsion coating weight and the silver halide/gelatin ratio. The maximum useful range is determined by the emulsion thickness; furthermore, the electron is most effective in producing developable grains when its range is slightly less than the emulsion. Unlike photons, which produce their greatest effect near the emulsion surface, electrons produce the most grains after slowing below a threshold energy.

A relatively energetic electron has little photographic effect; its ionizing ability is high, but it passes

by grains near the film surface too rapidly to cause a developable grain (excluding knock-on electrons). As it progresses through the emulsion, it loses energy and slows down. If its track ends near the rear of the emulsion, the parameters of speed and Dmax will be at a maximum. The broadness of this maximum and the continued response afterward are due to both oblique scattering of electrons and direct hits followed by secondary electrons. The minimum response occurs when the electron cannot penetrate the emulsion (5-7 KV). The spectral sensitivity maximum lies between 50-75 KV for most emulsions, but since it is a function of coating weight, the maximum can be shifted to some extent by the manufacturer.

A closely allied phenomenon is reciprocity failure. This is evidenced by the density differences resulting when equal exposures are made at different intensity levels. It is caused by the difference in arrival times between the quanta required for developability. The occurrence of grains made developable by a single electron precludes any time difference between quanta so that for these grains there is no failure. Grains requiring more than one electron are subject to reciprocity failure and this has been observed (Mees and James, 1966, p. 183). Although this area has not been investigated completely, it appears that reciprocity failure for electrons occurs mainly at the higher densities, in large grained emulsions, and with

exposure times on the order of 0.1-5.0 sec (Digby et al., 1953; Mees and James, 1966, p. 183). In most recording applications the emulsions would be fine grained and exposure times would be less than 0.1 sec.

Modulation Transfer Function

The major difference between photon and electron MTFs arises, as in the previous section, from the differing modes of energy penetration. Photons are most effective near the emulsion surface while electrons are most effective near the end of their track. This causes fundamental differences in the emulsion spread function or its Fourier transform the MTF.

The spread function for electron exposed emulsions generally depends on the electron range, a function of electron energy, and emulsion coating weight (Mees and James, 1966, p. 183). Between the limits of low energy electrons which do not penetrate the emulsion and high energy electrons with ranges greater than the emulsion thickness, electrons scatter in a roughly hemispherical region (see Figure 2). If this scatter were a true diffusion process then the spread function density profile would be Gaussian with the form of:

$$S(x) = (b)e^{-(x^2/2\sigma^2)} \qquad (6)$$

where $S(x)$, the density, falls to 5% of the peak, b, at a width of 4σ (Valentine, 1966). Freiser and Klein (1958)

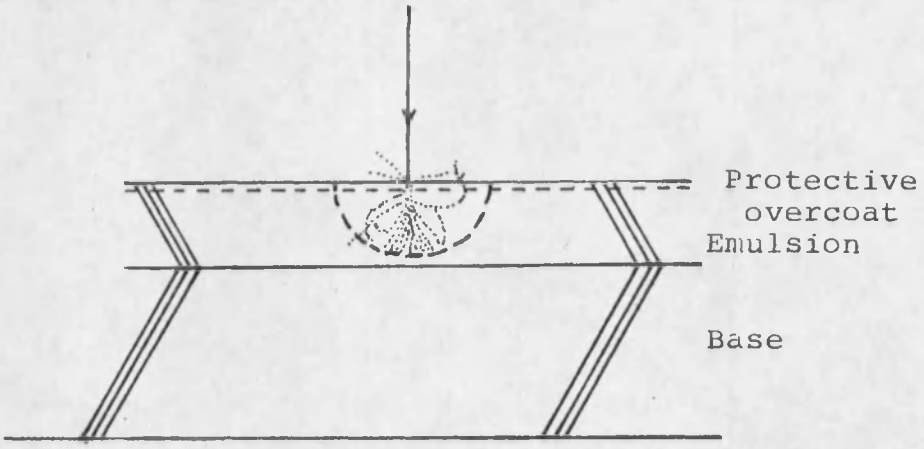

Figure 2. Visualized electron scatter -- Dots indicate electron path after impact; circular zone indicates electron range.

find, however, that a better fit to experimental data is obtained with the functional form of:

$$S(x) = (b)10^{-2|x|/k} \tag{7}$$

where k is the width of the function at 10% of the peak. The Fourier transform of this $S(x)$ with s as the spatial frequency variable is then:

$$F(s) = \frac{1}{1 + (0.43\pi ks)^2} \tag{8}$$

with $F(s)$ as the modulation transfer function.

Tarnowski and Evans (1962) appear to have verified the form of this transfer function down to 20 KV electrons. Additional confirmation appears in the work of Burge and Garrard (1968). They examined a modified form of the spread

function as given by Freiser and Klein (1958) along with the Gaussian form and a "bell-shaped" form. They found that the Freiser form provided a good fit for electrons of 7 and 60 KV energies. Values of the parameter k as reported by Freiser and Klein (1958) and Valentine (1966) and as calculated from Tarnowski and Evans (1962) and Burge and Garrard (1968) are tabulated in Table 1.

The very low value of 2.3 μm for k as calculated from Burge and Garrard (1968) represents the limits of their measuring instrument. This value corresponds to 960 cycles/mm at 10% modulation. The value of 4.6 μm corresponds to 480 cycles/mm at 10% modulation; according to Tarnowski and Evans (1962) this value can be attained in actual recording applications by keeping the beam diameter below 1.3 μm. Such low values for k are not representative of standard electron microscopy, where 50 KV and higher voltage electrons are used. Low voltage electron recording appears to offer the advantage of high resolution.

In summary, the principal characteristics of electron exposed emulsions (excluding granularity characteristics) are: a linear D-E curve with convenient descriptors of speed and Dmax, a spectral sensitivity curve which may be altered slightly during manufacture, a lack of reciprocity failure in most recording applications, and a modulation transfer curve extending to 500 cycles/mm for

Table 1. Reported values for the parameter k.

Source	Emulsion Type	Emulsion Thickness (μm)	Emulsion Density (g/cm)	Electron Energy (KV)	Electron Range (μm)	k (μm)
F	22	13.4	0.59	52	16	28
	22			68	26	27
	22			82	38	26
	23	22.4	0.59	52	16	28
	24	31.3	0.59	68	28	35
	25	53.9	0.59	82	38	60
V	N60	15	-	60	-	6.5
	-	25	-	60	-	40
T	HRP	-	-	14	-	4.6
	HRP			20		10
	HRP			30		12
	HRP			50		20
	SER	-	-	20	-	4.6
B	SLC	13	0.85	60	-	28
	SLC			40		13
	SLC			7.3		2.3
	G5	10.5	3.16	60	-	16
	G5			7.3		2.3
	DC3	2	-	60	-	11
	DC3			7.3		2.3

Sources are: F, Freiser (1958); V, Valentine (1966); T, Tarnowski and Evans (1962); B, Burge and Garrard (1968). Emulsions are: 22-25, sample research coatings; N60, G5, Ilford Nuclear Research Emulsions; SLC, Ilford Special Lantern Contrast; SER, a special electron recording emulsion; HRP, Kodak High Resolution Plate; DC3, Kodak C type emulsion.

low voltage applications. The next section examines the granularity or noise involved in such recording.

Emulsion Noise Properties

As with most communication channels, the high frequency response of photographic emulsions is finally limited by grain noise. There are two descriptors typically used to characterize noise, the auto-correlation function and the Wiener (or power) spectrum of the noise; these two functions are related by a Fourier transform. Although the Wiener spectrum is quite useful for estimating the effect of photographic noise in various applications (R. C. Jones, 1955; Doerner, 1962; Zweig, 1956), obtaining this spectrum requires on the order of 10,000 data points to achieve 20% accuracy (Bendat and Piersol, 1966, p. 206), and the spectrum obtained may not truly characterize the material due to the measuring instrument and material interaction.

The measure which has been typically used to evaluate film noise is the so-called Selwyn Granularity Coefficient (Selwyn, 1935). This measure, supposedly independent of the measuring instrument, was originally defined as:

$$G = \sigma(D)\ (2a)^{\frac{1}{2}} \tag{9}$$

where $\sigma(\underline{D})$ is the standard eeviation of the density, $\underline{D}$, around some mean $\overline{\underline{D}}$ measured with an aperture of area $\underline{a}$ (often the factor $(2)^{\frac{1}{2}}$ is dropped for simplicity). If in

addition it is supposed that $\sigma(\underline{D}) \propto (\underline{D})^{\frac{1}{2}}$, the definition can be further modified to:

$$G' = \sigma(D) \ (2a/\overline{D})^{\frac{1}{2}}. \tag{10}$$

In t is last form $\underline{G'}$ is presumed to be independent of both $\underline{a}$ and $\overline{D}$.

There are several theoretical derivations that relate $\sigma(\underline{D})$ to the measuring aperture, $\underline{a}$, to the number of grains in that aperture, $\underline{N}$, to the mean grain size, a', and to the density, $\underline{D}$ (Mees and James, 1966, p. 74). Starting with an unspecified number of grains, assumed to be completely opaque and allowing overlapping, then the grains obscure an area, A, within the measuring aperture. The transmission, $\underline{T}$, through the aperture is then:

$$T = (a-A)/a \tag{11}$$

and the density is:

$$D = -\log_{10}(a-A)/a. \tag{12}$$

As the aperture explores the emulsion a different obscuration is observed leading to a change of density:

$$dD = 0.434 \ dA/(a-A) \tag{13}$$

valid for small changes in $\underline{T}$. If there were no overlapping then:

$$dA = a \ dN; \tag{14}$$

however, allowing overlapping, it can be argued that:

$$dA = T \ a \ dN. \tag{15}$$

While true in the limits of $\underline{T} = 0$ and $\underline{T} = 1$, two grains which overlap can be expected to absorb less light than two grains (opaque) in separate areas. This is examined by Bayer (1964).

Continuing by substituting (11) and (15) into (13) and integrating, then:

$$D = 0.434\ N\ (a'/a) \tag{16}$$

and the noise, $\sigma(\underline{D})$, can be found as:

$$\sigma(D) = (0.434\ \overline{D}\ a'/a)^{\frac{1}{2}}; \tag{17}$$

therefore, the Selwyn granularity is then:

$$G = (2a')^{\frac{1}{2}}(0.434\ \overline{D})^{\frac{1}{2}}. \tag{18}$$

The assumption treating overlap in Equation (15) above leads, according to Bayer (1964), to a $\sigma(\underline{D})$ which is too low. He finds that, excluding the low density region, $\sigma(\underline{D})$ should be increased by a multiplicative factor depending on the grain size/aperture ratio, $(\underline{a}'/\underline{a})$, and the optical density. This factor is approximately:

$$F = 1 + 0.23(\overline{N}a') - 0.58(a'/a)^{\frac{1}{2}} + \ldots \tag{19}$$

Then the corrected $\sigma'(\underline{D})$ will be:

$$\sigma'(D) = F\sigma(D). \tag{20}$$

The factor $\underline{F}$, is approximately equal to 4 for a density of 3 and a "usual" value of $\underline{a}'/\underline{a}$. Bayer, however, mentions in his conclusion that although the correction factor is

significant, in a real situation it may not be as significant due to the illuminating cone angle and emulsion scattering.

Another assumption in the derivation is that of equi-area grains. Haugh (1963) treats this by partitioning the various grain sizes into classes with a class area of $\underline{a}'_i$ and a class average number of $\underline{N}_i$; the grain area used in the derivation of (18) then becomes a special, area-weighted average defined as:

$$a'' = \sum_{i=1}^{\infty} (N_i a'^2_i) / \sum_{i=1}^{\infty} (N_i a'_i). \qquad (21)$$

Since as exposure increases a larger fraction of smaller grains becomes developable, this average, $\underline{a}''$, will vary with exposure. Haugh could not find a clear relationship between the emulsion characteristic curve and the value of $\underline{a}''$.

Marathay and Skinner (1969) sidestep this problem in a different formulation of the grain size-sensitivity distribution. They find that the different sensitivities result in a model with a lower granularity than the model represented by Equation (18) and corrections.

Experimental Granularity Measurements

In the final analysis, although the Selwyn model does not represent granularity as a constant independent of the measuring instrument and emulsion, it nevertheless is a

close approximation over certain limited aperture sizes. In attempting to find an objective measure of granularity correlating with the subjective measure, Jones and Higgins (1946) evaluated $\underline{G}$ for several apertures, films, and density levels. This experiment suffered from inadequate sampling, too few data points. R. C. Jones (1955) attempted to fit a theoretical Wiener spectrum to the data of Jones and Higgins (1946). This curve, a function of $\underline{\bar{r}}$, the average grain radius (circular grains); $\underline{D}$, average density; and $\underline{Q}$, the opacity of a single grain, results in an equation:

$$\Phi(s) = a' \log_{10} e \, \bar{D} \, Q[J_1(2\pi s\bar{r})/\pi s\bar{r}]^2 \qquad (22)$$

where $\underline{a}'$ is the grain area and $\underline{J_1}$ is the first order Bessel function. From the photomicrographs of Jones and Higgins, he found that $\underline{\bar{r}} \simeq 0.75\mu m$ and $\underline{Q} \simeq 0.8$. The spectrum thus determined did not even approximately resemble the derived spectrum. To match the derived spectrum adjusted values of $\underline{r}$ and $\underline{Q}$ were used: for $\underline{\bar{D}} = 0.28$, $\underline{Q} \simeq 0.164$ and $\underline{\bar{r}} \simeq 4.0\mu m$; and for $\underline{\bar{D}} = 1.76$, $\underline{Q} \simeq 0.0176$ and $\underline{\bar{r}} \simeq 16.0\mu m$. From the arguments previously given by Haugh (1963) the increase in $\underline{\bar{r}}$ is not surprising; however, at the higher density $\underline{\bar{r}}$ has increased again which is opposite to Haugh's theory.

Some of this may be due to the original inadequate sampling; the grain clumping as noted by R. C. Jones (1955) is certainly due to the sampling. This was pointed out by

Zweig (1956). He determined the autocorrelation functions for several emulsions. Clumping would tend to add a tail to the autocorrelation function and thus add peaks in the low frequency region of the Wiener spectrum. Zweig demonstrates that this tail tends to disappear as the number of measurements increase. In particular, he points out that many previous determinations of $\sigma(\underline{D})$ were based on as few as 200 to 300 measurements, and that to determine $\sigma(\underline{D})$ with 95% confidence about 800 measurements are required. Therefore, the results of Jones and Higgins (1946) are of doubtful validity.

In addition to the problem of inadequate sampling, Zweig (1956) points out that the measuring system numerical aperture strongly influences the evaluation of $\underline{G}$. The truncation of the effectively flat Wiener spectrum of the film distorts the probability distribution of density and therefore $\underline{G}$ will not be instrument invariant.

He also points out that, in any small region of the plot of log $\underline{G}$ against log $\underline{a}$, the curve is essentially linear but that the slope (exponent of $\underline{a}$) is less than $\frac{1}{2}$. This implies that in order to maintain the form of the formula for $\underline{G}$, a slightly larger "effective" aperture should be used. This aperture may be the actual system aperture corrected for aberrations or defocus.

Finally, he examines the effect of drift in the microdensitometer and macroscopic density variations

(wedging) within the scanned region. Both of these effects must be much lower than $\sigma(\underline{D})$ during the period of measurement.

The next extensive evaluation of granularity, by Higgins and Stultz (1959), took these points into consideration. Using a more accurate and rapid instrument than in 1946, they tested several film, aperture, and density combinations. This time they found fewer variations of $\sigma(\underline{D})$ $\underline{vs}$ $\underline{a}^{\frac{1}{2}}$, but some variation still remained, especially with large apertures. Although not specifically mentioned, if the data are plotted, $\log \sigma(\underline{D})$ against $\log \bar{\underline{D}}$, there appears to be good agreement with $\sigma(\underline{D}) \propto \bar{\underline{D}}^{\underline{p}}$ but the exponent $\underline{p}$ varies from film to film. It does not appear to vary with the aperture except for $\underline{a} > 300\mu m$. The value of $\underline{p}$ was between 0.30 and 0.45 with the larger value associated with the finer grained material.

Granularity for Electron Exposure

The granularity of silver halide materials exposed to electrons will not necessarily permit the assumption that $\underline{G}$ should be constant. As mentioned in the section on the macroscopic emulsion response, one electron has sufficient energy to expose several grains; hence the electron beam noise is effectively multiplied by the film. This multiplication takes place along the electron path and causes the formation of grain aggregates. Since these

aggregates represent grain clumping, the noise spectrum of the material for electron exposure will exhibit a low frequency peak. For that reason, Selwyn's (1935) relationship may not be valid.

A similar "clumping" occurs with light exposures, the mottle found in enlarged prints. Stultz and Zweig (1959) have examined Selwyn's relationship in the presence of such mottle. They assign a $\sigma(\underline{D})_m$ to the variation due to the mottle and a $\sigma(\underline{D})_g$ to the primary grain variation; the measured variation then becomes:

$$\sigma^2(D)_{measured} = \sigma^2(D)_m + \sigma^2(D)_g. \qquad (23)$$

Theoretically, as the scanning aperture, $\underline{a}$, becomes smaller the variation $\sigma(\underline{D})_g$ becomes larger and $\sigma(\underline{D})_m$ smaller; then, in the limit $\underline{a} = 0$, the measured variation is effectively $\sigma(\underline{D})_g$. Conversely, for large apertures the measured variation is caused primarily by $\sigma(\underline{D})_m$. In practice when they plotted log $\sigma(\underline{D})$ against log $\underline{a}$, they observed two displaced regions each with a slope of $\sim\frac{1}{2}$. In the two regions Selwyn's relationship was approximately valid and the size of the primary grain and grain "clumps" could be estimated. This may be a valuable tool for analyzing "clumping" in enlarged prints but it has not been verified for the clumps caused by electron exposure.

The model for granularity in electron exposed emulsions has not been developed fully. Presently there are

two models in use; the first, proposed by Valentine (1965, 1966), considers the granularity to be dependent on three variables which are assumed independent events within the small measuring aperture, $\underline{a}$. Thus the noise is described as:

$$\left(\frac{\sigma(D)}{D}\right)^2 = \left(\frac{\sigma(E)}{E}\right)^2 + \left(\frac{\phi(\phi)}{\phi}\right)^2 + \left(\frac{\sigma(a')}{a'}\right)^2 \qquad (24)$$

where $\underline{E}$ is the exposure, ϕ is the number of developed grains per electron, and $\underline{a'}$ is the grain area. Relating each factor to $\underline{M}$, the average number of electrons received in the area $\underline{a}$, and ϕ, he arrives at the expression,

$$\frac{\sigma(D)}{D} = \frac{1}{\underline{M}^{\frac{1}{2}}} (1 + 2/\phi)^{\frac{1}{2}} . \qquad (25)$$

Since for electron exposures, $\phi > 1$, the input noise, $\underline{M}^{\frac{1}{2}}$, is multiplied by a factor less than 2. For photon exposures $\phi < 1$; therefore, the input quantum noise is multiplied by a factor greater than 2. It should be noted, however, that in a typical emulsion more photons than electrons are required to produce the same density; hence, the photon input noise is smaller.

However, a photon exposed emulsion represents an inefficient recorder; a "perfect" recorder would produce an observable for each quanta input. R. C. Jones (1955) treats this by defining a "detective quantum efficiency" relating the input signal to noise ratio, $(\underline{S}/\underline{N})_i$, to the output $(\underline{S}/\underline{N})_o$. That is:

$$DQE \equiv (S/N)_o^2/(S/N)_i^2 . \qquad (26)$$

A perfect recorder has a DQE = 1. Photon exposed silver halide emulsions have a typical DQE of 10^{-3}; most of the electron exposed emulsions examined by Valentine (1965) and Valentine and Wrigley (1964) had DQEs approaching one. Some emulsions, the slow, fine-grained ones, did not have as high a DQE. These emulsions had DQEs between 0.3 and 0.02; the electron speed value ranged over a factor of 3.

These results tend to indicate that for some emulsions Valentine's (1965) model is invalid. This may be especially true for emulsions exposed to low voltage electrons. Burge and Garrard (1968) found that as the acceleration voltage was reduced from 60 to 7 KV the DQE decreased by a factor of 2 to 30 for the four tested emulsions.

Another model, which is based on empirical evidence and theoretical considerations related to print granularity, has been proposed by Freiser (Freiser, 1958; Freiser and Klein, 1958; Freiser, Klein, and Zeitler, 1959; Zeitler and Hayes, 1965). The measured granularity for small apertures is expected to be that of the primary grains, or that granularity expected for photon exposures, $\sigma(\underline{D})_p$. The granularity measured with large apertures consists of the contribution, $\sigma(\underline{D})_a$, due to the aggregates and the relatively small contribution due to $\sigma(\underline{D})_p$. Freiser (1958) states that:

$$\sigma^2(D)_a = \sigma^2(D)_p \phi \qquad (27)$$

where ϕ is the grain/electron ratio. This leads to an inequality valid for any aperture:

$$\sigma^2(\underline{D})_p < \sigma^2(D)_e \leq (\phi+1)\sigma^2(D)_p \qquad (28)$$

where $\sigma(\underline{D})_e$ is the measured variation for electron exposure.

Since Selwyn's relationship is not valid except for the extreme apertures, Freiser proposes a function, $\beta(\underline{a},\phi)$, which is a one parameter measure of granularity expressing the dependence of the aperture and grain/electron ratio. For small apertures or small values of ϕ, then $\beta \to 1$; usually $\beta(\underline{a},\phi) \leq 1$. For low densities ϕ is simply related to the emulsion speed by:

$$\phi = \frac{\varepsilon}{0.434\ a'} \qquad (29)$$

where ε, the speed, is defined by:

$$\varepsilon = \left.\frac{dD}{dE}\right|_{E \to 0} . \qquad (30)$$

Then over the region where the D-E curve is linear, β is independent of density. Hence:

$$\sigma^2(D)_e = \beta^2(\phi+1)\sigma^2(D)_p . \qquad (31)$$

As with the previous model, there are some practical difficulties with the model of Freiser (1958). It would seem that the inequality pertaining to the variance of the electron exposed material would indeed hold; however, the correction factor β would seem to be related to the

densitometry through its dependence on the aperture. At any rate, the factor β has not been well determined for any range of emulsion types.

In addition, there is some disagreement in the typical range of ϕ for various emulsions. Freiser and Klein (1958) found values of ϕ between 5 and 50 grains/electron; Valentine (1966) states that these values appear large. He finds that an overestimate of ϕ can be made via:

$$\phi \simeq \frac{3}{2} R \, (F/2r)$$

where $\underline{R}$ is the electron range; $\underline{F}$, the silver halide/gelatine ratio; and $\underline{r}$, the grain radius. Using this formula for NT4 plates ($\underline{F} = 0.5$, $\underline{r} = 0.15\mu m$, $\underline{R} \cong 25\mu m$) gives $\phi \simeq 50$ grains/electron. Actual grain counting gives $\phi \simeq 25$ grains/electron. Further, he finds that for the emulsions tested ranged from 2 to 20 grains/electron. Hamilton and Marchant (1967) in their evaluation of Kodak Electron Image plates found that their theoretical curves fit best with $\phi = 4$ grains/electron, while grain counting revealed 6 grains/electron. That model, which appears to result in a more complete (but fairly intractable) expression for $\sigma(\underline{D})_e$, will not be discussed.

Aside from a few data points to exhibit these three models, there seems to be almost no reported data on electron granularity, especially the variation of granularity with density. The existing published data often

suffer from inadequate sampling (i.e., statistical uncertainties) or too few levels of density, or both.

Tajima (1958) obtained curves for Selwyn granularity against density for light and 50 KV electrons. From 5 density levels for electron exposures and 3 levels for light he found that $\underline{G} \propto \underline{D}^{0.35}$ for both light and electron exposures. He also reports values for $\sigma(\underline{D})$ at a density of 0.49 ± 0.02 using a 5 by 500μm aperture; they are:

Energy:	light	50KEV	70KEV	130KEV
$\sigma(D)$:	0.0185	.0242	.0250	.0232

In view of the apparent statistical uncertainty in the given value of density, it is difficult to find significant differences in the values for $\sigma(\underline{D})$.

A more complete experiment by Morimoto, Mori, and Sobue (1962) reports that $\underline{G} \propto \underline{D}^{1.0}$ and $\underline{D}^{0.91}$; for the 50 KV electron exposure the value of ϕ was 1.4 grains/electron; the ratio, $\sigma(\underline{D})_e/\sigma(\underline{D})_p$, ranged between 1.18 and 1.29 increasing with electron energy. Although the experiment tested several variables, the statistical uncertainty is large; only 100 independent data points were taken, but 600-800 are required for 95% confidence in $\sigma(\underline{D})$.

This statistical confidence is available in the experiment by Burge and Garrard (1968). They evaluated $\sigma(\underline{D})$ and the autocorrelation function, ϕ, using 1200

measurements at intervals of 0.8$\underline{r}$ ($\underline{r}$, the circular aperture radius); this gave about 600 independent samples.

They examined the variation of: $\sigma(\underline{D})$ with $\underline{r}$ for 6 levels between 3.3 and 33μm and a constant electron energy; and $\sigma(\underline{D})$ with electron energy for 2 levels, 7.3 and 60 KEV, at a constant measuring aperture, $\underline{r}$ = 22.5μm. Each test was at a constant $\overline{\underline{D}}$ = 1. They found no significant effects due to the microdensitometer objectives (N.A. = 0.10, 0.12, 0.25).

They reported results for 2 emulsions. No evidence of correlation (clumping) was found for G5 emulsion under any of the experimental conditions; SLC emulsion exhibited grain correlation over a distance of ∿15μm for 60KV electrons. They explain this paradox by presuming that "the developed grains in G5 cluster around the point of electron impact whereas those for SLC, which is much less rich in silver grains, are distributed over a larger area" (Burge and Garrard, 1968, p. 715). The results of the log $\sigma(\underline{D})$-log $\underline{a}$ curve show the correlation: for SLC $\sigma(\underline{D}) \propto \underline{a}^{-0.37}$ and for G5 $\sigma(\underline{D}) \propto \underline{a}^{-0.45}$. Values for the variation of $\sigma(\underline{D})$ with electron energy for $\underline{a} = 1600\mu m^2$ are:

σ(D)	60KEV	30KEV	7.3KEV
SLC	0.032	0.024	0.014
G5	0.055	0.038	0.018

Using numerous assumptions Burge and Garrard (1968) calculated the theoretical $\sigma(\underline{D})$ using the formula given by Hamilton and Marchant (1967); the results were quite close to the experimental results (experimental results lower by 10-20%). Using values for speed and ϕ from Burge, Garrard, and Browne (1968), $\sigma(\underline{D})$ can be calculated by Valentine's (1966) formula; they are

$\sigma(D)$	60KEV	30KEV	7.3KEV
SLC	0.029	0.025	0.007
G5	0.045	0.027	0.015

These values are lower than the experimental values by 10-20%. Since neither of the two formulas predict with an error less than 10-20%, then either may be used; Valentine's formula is much easier to apply.

Summary

The data presented indicate that there is no satisfactory model treating electron exposure granularity. This seems to be the result of inadequate data or uncertain data covering too few experimental levels, especially for the density variable.

The microdensitometer used to measure the granularity can be a cause of the discrepancies reported in the literature. Microdensitometer considerations are beyond the scope of this paper; however, some explanations of the

failure of Selwyn's relationship involving microdensitometry, particularly regarding sample illumination and partial coherence, may be found in Zweig (1956), Kraus (1968), and Vernier (1969).

The data presented in the following sections are then microdensitometer specific. They are also from a single coating of a special, extremely fine grained electron emulsion. The selected apertures, hopefully, are representative of the anticipated usage of the emulsion.

CHAPTER 3

EXPERIMENTAL PROCEDURE

Electron Exposures

The electron exposures were made using a Phillips EM-75B electron microscope. The instrument had been modified to use an external Phillips PMR high voltage power supply which provided a metered acceleration voltage variable between 0 and 75 KV. The installed high voltage meter was assumed correct; for the meter ranges used, the estimated voltage reading error was 5%. The microscope consists of three lenses, condenser, objective, and projector, the power of each controlled at the instrument control panel. At the voltages used the lenses were not capable of forming a reasonably unaberrated image; they were capable of forming a uniform beam. The filament was operated at various currents (depending on the vacuum available) between 5 and 40μa, where an automatic cut-off would turn off the high voltage. Normally, when the microscope is used at voltages between 40-75 KV, the filament is driven to saturation (space charge limit between the wire filament and the grid cup). This stabilizes the output intensity, but it could not be done at the low voltages used. Due to the anticipated problem of beam instability,

the intensity was measured before and after each exposure. The maximum variability was 20%, the average less than 5%. The microscope is diagrammed in Figures 3 and 4 and the complete instrument is illustrated in Figure 5.

Exposure intensity was determined with a detector located in place of the microscope viewing screen (see Figures 6, 7, and 8); this location receives 1/9 of the intensity on the film (determined geometrically). The detector is diagrammed in Figure 9. The 3-in diameter shield isolated the Faraday cup from external charge effects and was coated with a phosphor to permit viewing the beam. The current between the cup and ground was measured with a Hewlett Packard HP-425 picoammeter.

The cup, however, was too small for measurements at high magnifications, due to the low current. It had been designed to detect the current at a low magnification; this current was to have been extrapolated to a higher magnification. Unfortunately, the relationship between magnification and current density could not be determined well enough to allow the extrapolation. For this reason measurements were taken using both the cup and the shield as electron collectors. This method can cause considerable error due to the electron-photon conversion in the phosphor, the unavoidable reflection and secondary electron emission, and the repulsion effects caused by local charging of the walls around the detector.

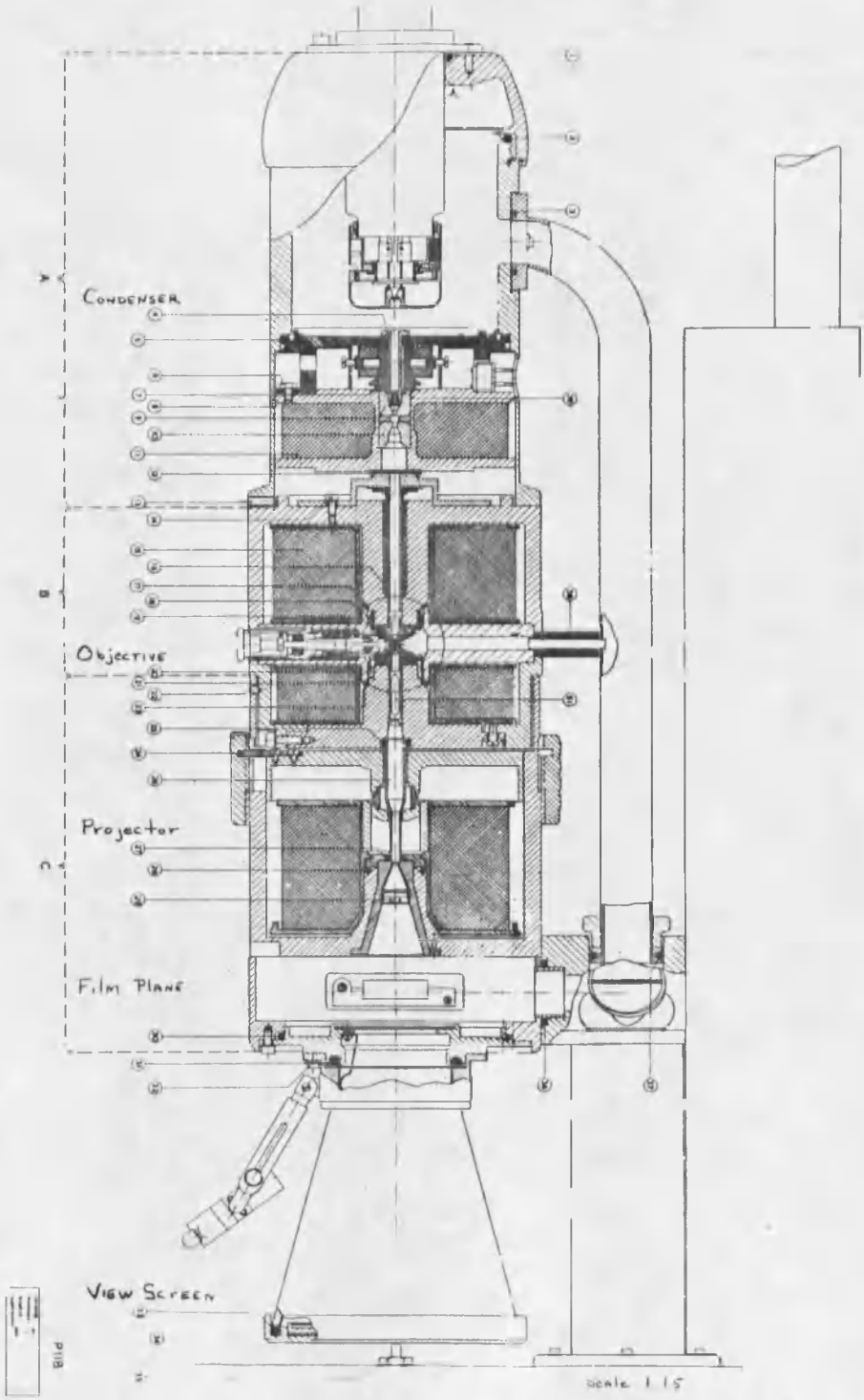

Figure 3. Electron microscope schematic.

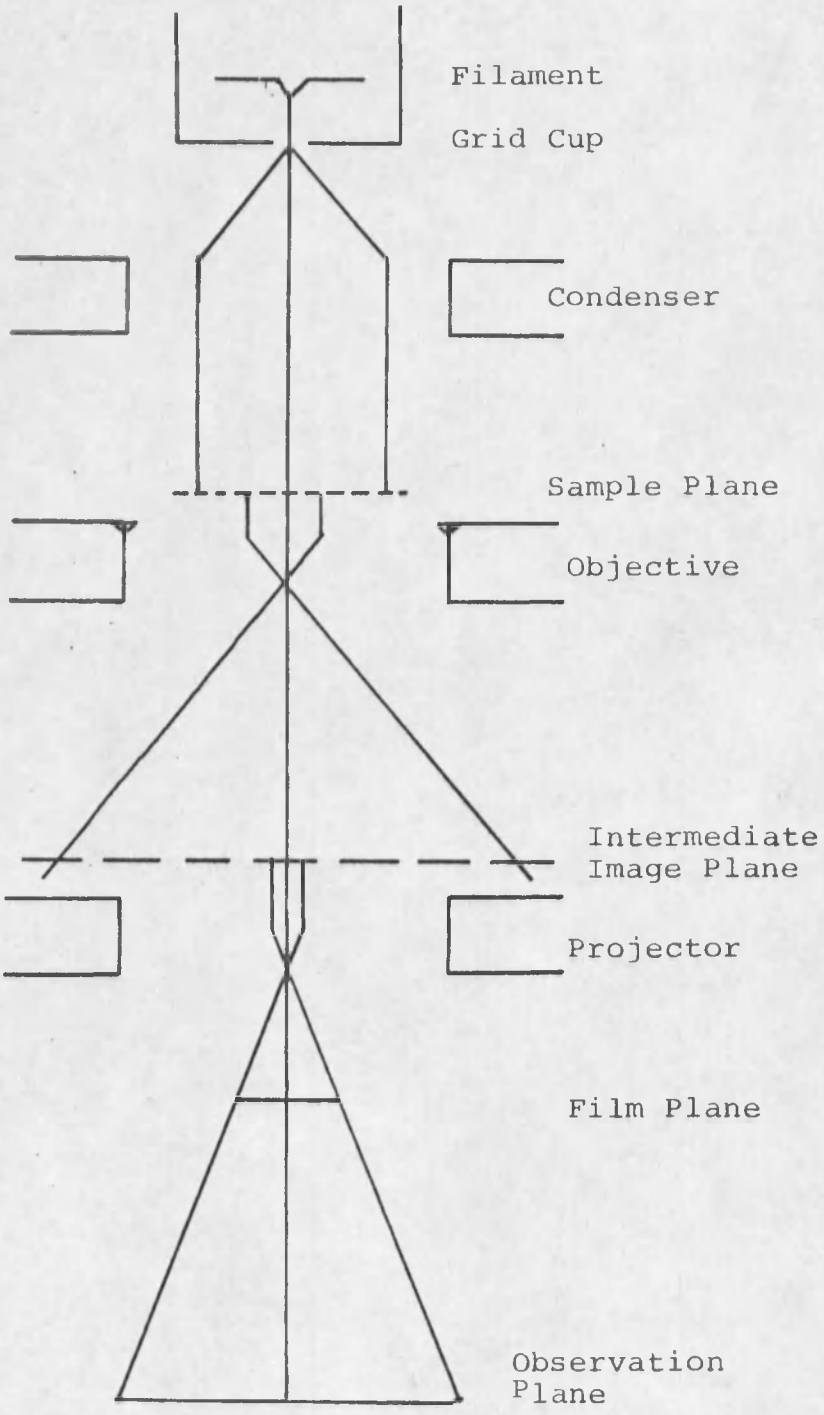

Figure 4. Electron path in EM75B microscope.

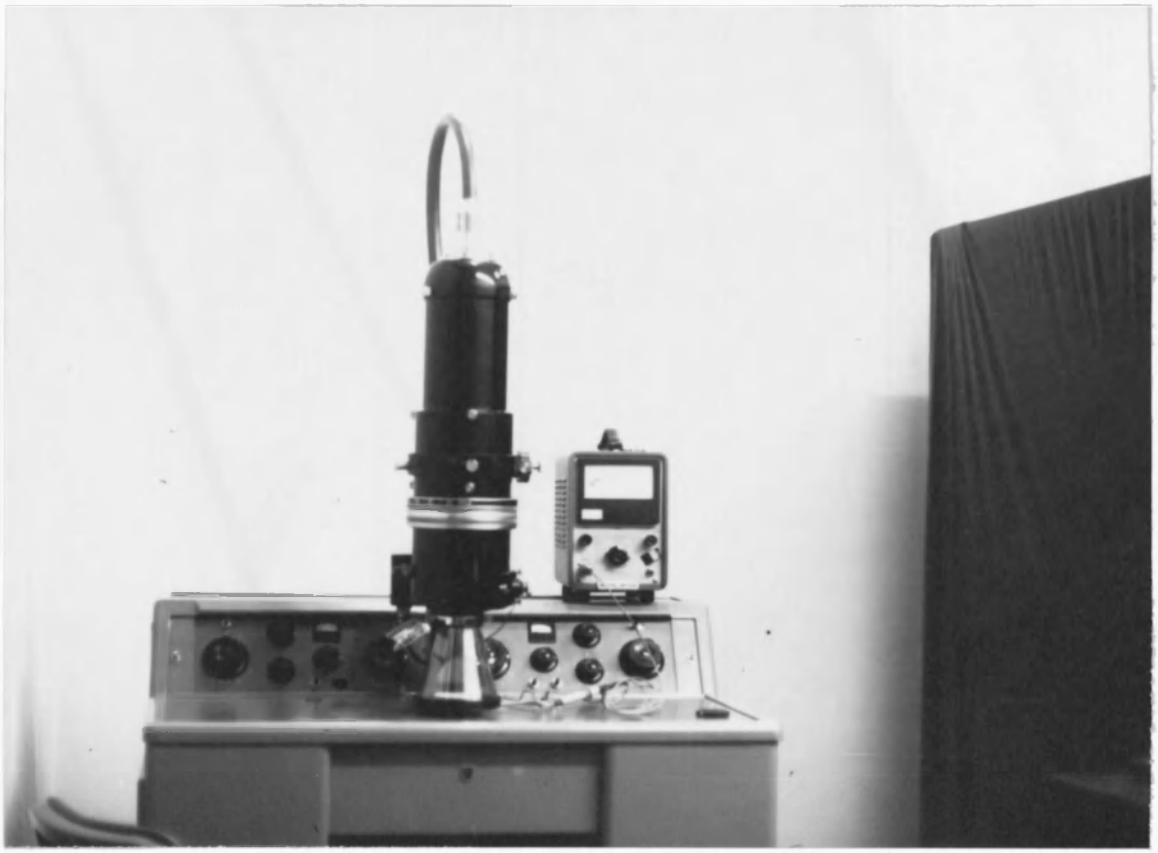

Figure 5. Photograph of electron microscope.

Figure 6. Microscope instrumentation.

Figure 7. Electron detector installed.

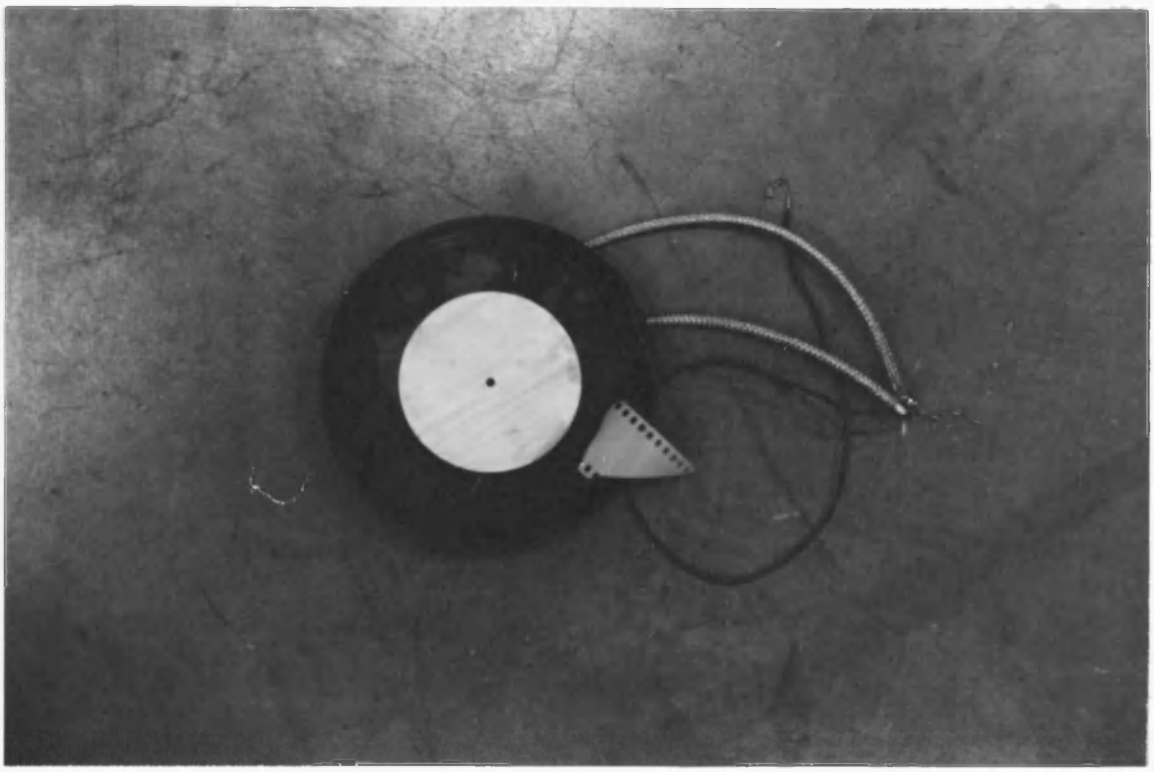

Figure 8. Electron detector top view.

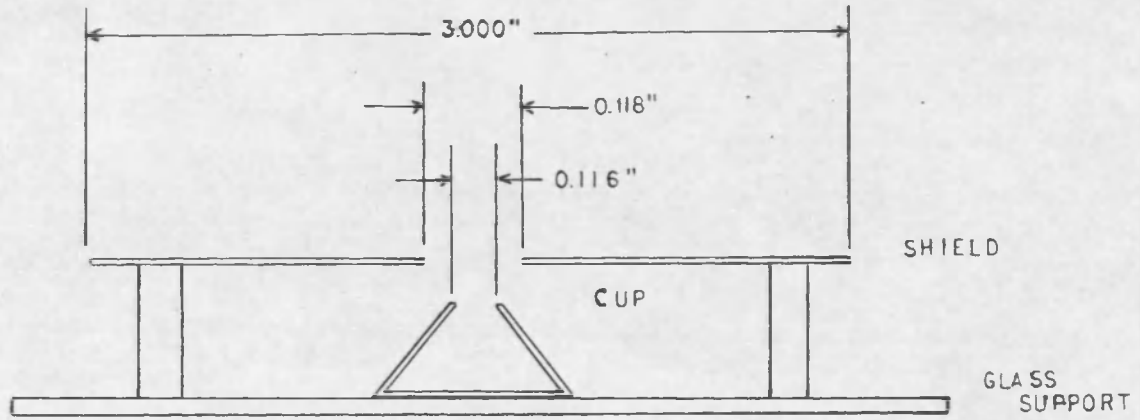

Figure 9. Faraday cup electron detector

In order to reduce these errors an effort was made to establish the ratio between the currents detected by the large detector (cup and shield) and the small detector (cup). These data appear in Table 2. Geometrically, the large detector should collect 670 times the current collected by the small detector; the actual ratio is much less, as expected for the reasons discussed above. The variation in ratio with voltage is probably caused by changes in electron-photon conversion efficiency and the increased reflection at higher energies. It is considered insignificant for magnifications greater than 5.

The change in ratio with magnification is not the change expected by assuming that the product of the current density and the squared magnification is constant. Since the beam current density has a Gaussian profile, a more complete analysis is necessary; this was not attempted because at the higher magnifications some vignetting was expected. The ratio appeared to stabilize for magnifications greater than 5.

The best large/small detector ratio is then taken to be 130 for all voltages and for magnifications greater than 5. Since this value has an estimated error of 10%, all exposure values have the same error.

No problems associated with charge buildup were observed with the large detector. This effect can be observed as a decrease in output current with increasing

Table 2. Determination of large/small collector current ratios.

KV	Mag	I (in picoamperes) I-Large	I-Small	Ratio
	Shield grounded for small collector measurements			
20	1.5	24,000	165	140
	1.5	31,500	255	120
	3.0	6,800	58	120
	5.0	2,100	15	130
	7.0	1,400	10	140
15	1.5	46,000	470	98
	3.0	14,200	130	110
	5.0	4,600	38	120
	8.0	2,600	19	140
	11.0	1,400	10	140
10	1.5	84,000	1050	80
	3.0	27,000	320	84
	5.0	8,800	72	130
	8.0	4,500	35	130
	11.0	2,500	21	120
	Shield ungrounded for small collector measurements			
20	3.0	6,800	110/85[a]	61/80
20	5.0	2,100	38/30	55/70

[a]Second value taken 3 min after startup (first) value.

time; such an effect can be noted for the small detector with the shield ungrounded (last part of Table 2).

An attempt was made to find positions of the lens controls which would allow reliable, repeatable intensity control. This would allow a series of exposures differing in intensity rather than in time in order to avoid possible reciprocity effects. Such control was impossible to obtain, possibly because the lenses are not designed to operate with the low accelerating voltages used. Some lens control positions led to uneven intensity patterns particularly diffractions spots (high intensities at the center of the film in a radial star-like pattern). Once a group of settings was found that produced even intensities, the exposures were made. These settings changed slightly from hour to hour and were usually not useful the next day. This was complicated due to contamination in the microscope and the periodic necessity of adjusting the filament-grid spacing to obtain sufficient intensity. The microscope was disassembled for cleaning after about 3/4 of the exposure series had been done in order to maintain a sufficient level of intensity.

As a result of these problems, a time scale series of exposures was run. The current density varied between 5 and 200 pa/cm^2; the exposure times in all cases was greater than 10sec to reduce the timing error. Caution should be taken in extrapolating these exposures to the much higher

intensities and shorter times expected in an actual recording system.

Photon Exposures

The photon exposures were made using a 35w mercury penlight lamp. This was enclosed in a container with a 1½- by ¼-in slit; the container was attached to a meter stick. In order to obtain an intensity scale series of exposures in the limited area a step tablet was attached to the film with the sandwich m from the source. In order to determine the exposure in photons/cm^2, the source was filtered using a Wratten 50 filter which passes the blue 435nm line. Test exposures indicated that to cover the exposure range of the film times in excess of 24h were required. At this point the attempt to obtain the D-log E curve in photon units was abandoned; the curve obtained was an intensity series with an exposure time of 12h. With the step tablet and Wratten filter removed film Dmax could be obtained in 10s at 0.2m. This film is essentially insensitive in the visible spectrum. Kodak indicates that it has very little sensitivity beyond the blue (see Eastman Kodak Co., 1968). The exposures used for granularity scanning were made using the unfiltered source with times between 5s and 4min over distances between 0.2 and 1.0m. No attempt was made to determine the photon density since the spectral sensitivity of the film was unknown.

Processing

Each exposure set (about 30in) was developed in a double 35 Nikkor tank, one set per tank with an empty filler reel. The standard conditions were as follows: a short pre-wash to remove airbells, 5min Eastman Kodak D-19 or HRP developer agitated at 30s intervals, 3min water rinse, and 5min hardening fixer. This was followed by a 30min wash and a 30s Photo-flo treatment. Drying was by heated air for the electron exposed emulsions and by room temperature air for the photon exposures. Each solution was used once and discarded. All temperatures were 75 ± 2°F.

Densitometry

Diffuse density readings were made using a MacBeth TD402 densitometer with visual filter. These measurements were used to evaluate exposure uniformity in order to select the most uniform for later study. Diffuse densities were also used to obtain the D-E or D-log E curves.

Densities for the granularity determinations were obtained using a specially modified research microscope, the Zeiss Cytoscan (see Figures 10 and 11). Since there are very few of these modified microscopes in use, it will be discussed in detail.

The microscope was equipped with many selectable lenses; those of interest are listed below.

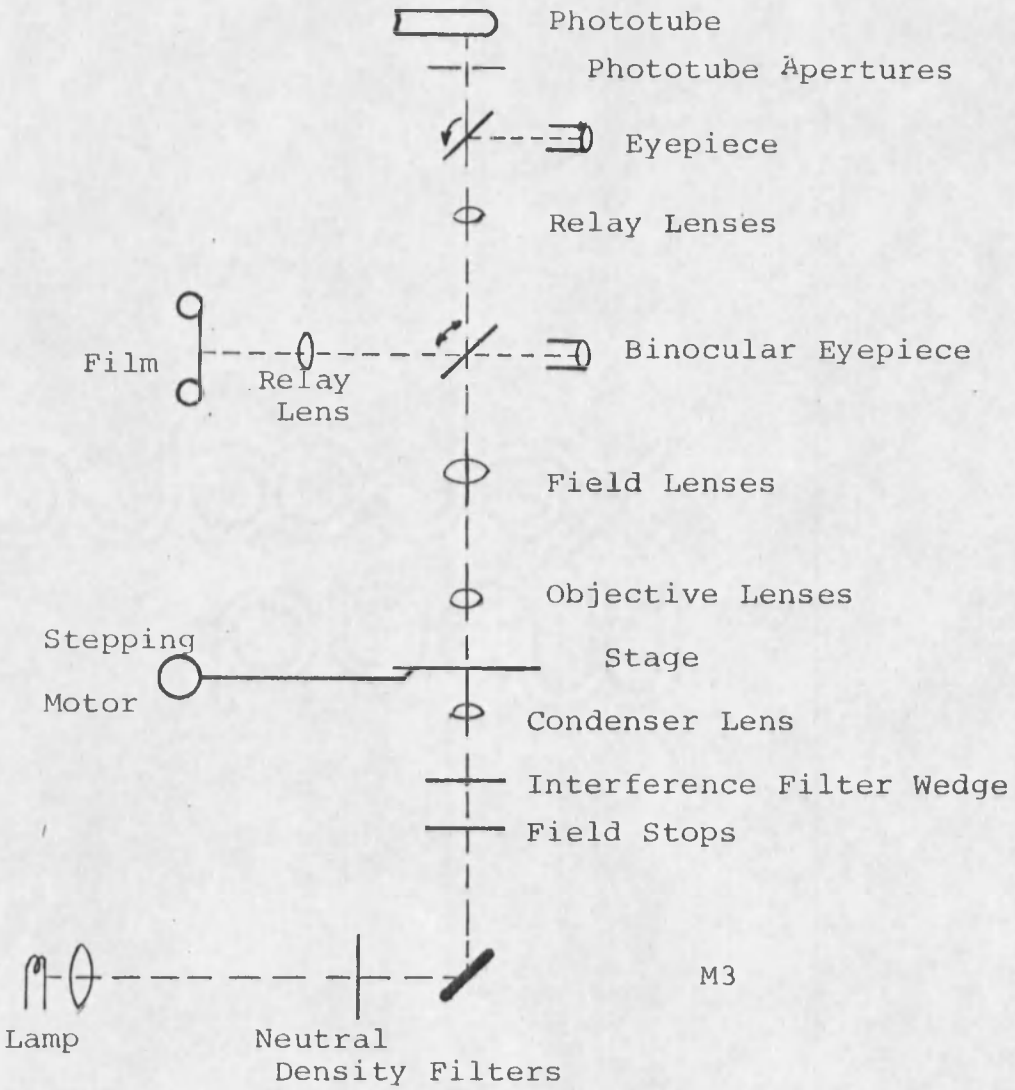

Figure 10. Simplified schematic of microscope.

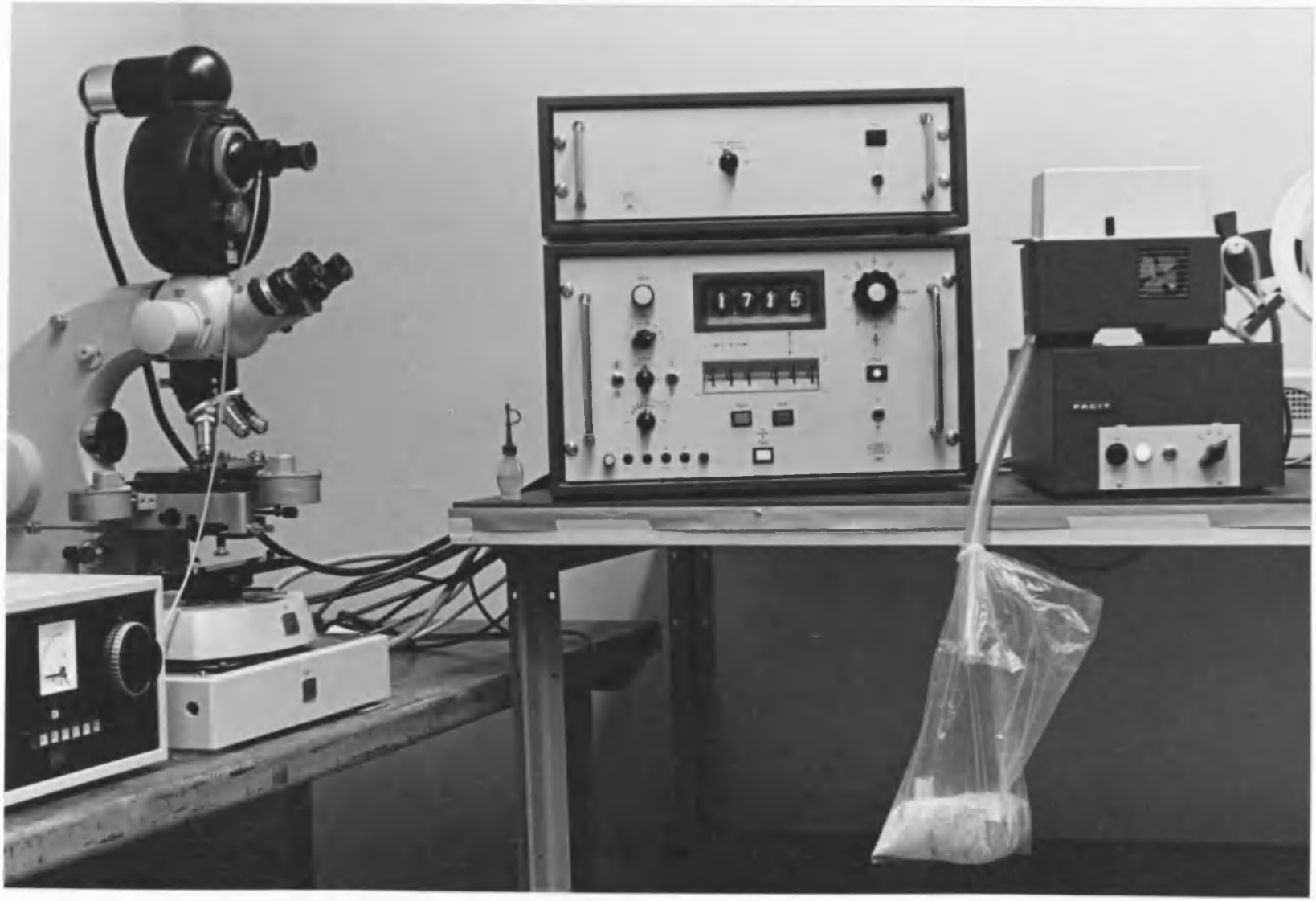

Figure 11. Zeiss microdensitometer.

Lens Location	Magnification	N.A.	Zeiss Type
Condenser	-	0.30	-
Objective	10X	0.22	Plan
Objective	16X	0.40	Neofluor
Objective	40X	0.75	Neofluor
Objective	100X	1.30	Neofluor-oil
Field	1.25X	-	-
Field	1.75X	-	-
Field	2.50X	-	-
Field	PH to observe objective exit pupil		
Phototube relay	10X	-	-
Phototube relay	20X	-	-
Phototube relay	10X UV	-	quartz lens

The 40X lens is corrected for a cover glass.

In the illuminating path prior to the condenser there are several neutral density filters which may be inserted into the path. These filters were found especially useful for adjusting the electronic zero density point (as discussed later); they had the determined values: 1.47, 0.87, 0.31, and 0.30 each ± 0.01 density. Following those there are several field stops, the smallest of which was about 0.1mm in diameter (approximately 1μm on the sample). Then there is a filter wedge which provides a choice of narrow wavelength bands across the spectrum; a clear area was used in this study for "white light" illumination.

The microscope stage has been modified to allow motion in two directions driven by stepping motors in addition to the usual vernier coarse movement. The stage movement has been interferometrically calibrated at the step increments of 0.25, 0.50, 1.00μm. As a consequence the stage vertical motion is limited to fine focus only;

therefore, the sample must be placed on the stage at approximately the correct object distance. This necessitated either mounting the film on a microscope slide or holding it on the slide.

Following the objective and field lens there are two mirrors; the first diverts the light to the binocular eyepieces or to an internal camera or to the second mirror. This second mirror diverts the light either to the photometer head or to a second eyepiece. The final stage fine focus was done while observing through this eyepiece.

The photometer head consisted of a RCA 1P28 phototube and a drum with 3 selectable apertures, 2 squares and 1 circle of nominal dimensions 1.25 and .625mm on a side and 1.8mm diameter. Knife edge traces made using the 16X, 1.25X, and 10X lenses (total magnification 200X) gave values of 1.75mm diameter and 1.2 and 0.8mm sides. These corresponded to 8.75, 6.0, and 4 0μm each ± 0.25μm on the sample.

The phototube output then went into a phase sensitive amplifier/rejection circuit. Since the lamp output was chopped at 120Hz, this circuit helped reject signals from the room lights and external sources. Following this the signal went into the control unit.

The control unit (Figure 12) contained the electronics for high voltage selection, stage step increment, dwell time or integration time for each step, total distance to be scanned, type of scan matrix (single line for

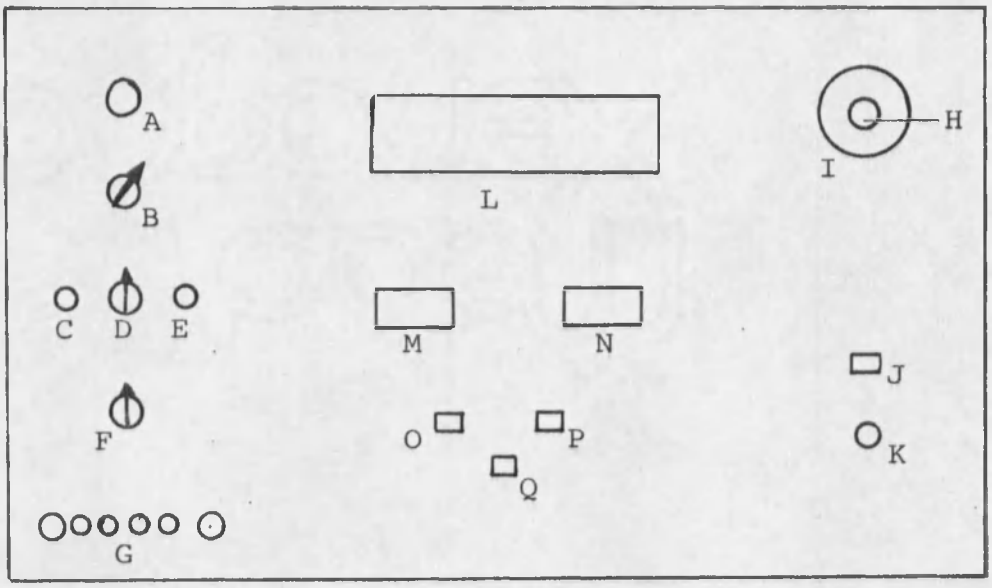

A--Density zero adjust
B--Point dwell (integrate) time switch
C--Scan line matrix switch
D--Point spacing (0.25, 0.5, 1.0μm) switch
E--Transmission/Density output switch
F--Output format switch
G--Transmission linearity trimpots
H--High voltage fine adjust
I--High voltage coarse adjust
J--AC power pilot
K--AC power switch
L--Output display
M--X total scan length selector
N--Y total scan length selector
O--Start scan switch
P--Stop scan switch
Q--Test switch

Figure 12. Scan control unit.

INPUT:

($\underline{i}$) lines of ($\underline{j}$) points - $\underline{d}_{ij}$ each point

CALCULATE:

1. Total ($\underline{ij}$) average $\overline{\underline{D}}$ and variance $s^2(\underline{D})$
2. Line average $\overline{\underline{d}}_i$ and variance $s^2(\underline{d}_i)$
3. Histogram of 25 cells each spaced at 0.01 density around $\overline{\underline{D}}$
4. Bartelett's test on each $s^2(\underline{d}_i)$
5. Overall average $\overline{\underline{d}}$ and variance $s^{-2}(\underline{d})$
6. Standard error on overall average $\underline{E}_d^2$ and variance $\underline{E}_s^2$
7. Variance $\sigma^2(\underline{d}) = s^{-2}(\underline{d}) + \underline{E}_d^2$
8. If $\underline{E}_d^2 > 10^{-1} s^2(\underline{d})$ reject or partition

Figure 13. Data reduction scheme

this experiment), switchable conversion from transmission to density (this experiment used only the density function), and output controller which selects either magnetic or punched paper tape.

The conversion electronics were limited to a maximum density of 1.73 and was highly nonlinear beyond a density of 1.5; between 1.5 and 1.3 the error was approximately 0.05 density units. This necessitated using neutral density filters in the microscope light path to provide a known zero offset in order to keep the conversion electronics from operating in the nonlinear region with samples of high density.

For example, assume that a sample with a density of 3 were to be scanned. After bringing the emulsion base into the microscopic field of view, three of the internal neutral density filters (totaling $\underline{D} = 2.08$) are added to the light path and the electronics are adjusted to read 100% transmission. The density transmission switch is moved to the density position (output is now $\underline{D} = 0$). Following this the neutral density filters are removed from the light path and the dense portion of the emulsion brought into view. The measured density is now about 0.92 and the scan is begun. The density fluctuations around this value do not depend on the absolute level selected as long as they are in the linear portion of the conversion curve (i.e., not more than 0.92 + 0.48 or -0.80). Following data reduction, the offset

density is added to the determined average. The effect of placing or removing filters from the light path and the effect of room lights on the measured granularity was tested using an analysis of variance technique. Neither effect was significant at a confidence level (alpha risk) of 0.05.

In order to zero set the instrument for the higher densities, the high voltage (gain) had to be increased, thereby increasing the noise. The instrument has provisions to reduce this noise by integrating longer on each point (increasing the point dwell time). For the high voltage setting used to measure a density of 1, there was no measurable noise at a dwell time of 0.135s/point. Increasing the gain to read a density of 3.5 with the same dwell time resulted in a noise level of 5×10^{-3} ($\sigma(n)$). For this reason, samples of high density were run with a dwell time of 0.5s/point where the noise was again below measurable levels. Samples with densities grater than 3.8 were not read because the low illumination levels made focusing impossible.

This ability to increase the point dwell time is not present in most microdensitometers, especially those which scan continuously. This one steps, stops, integrates for the selected time (from 0.03 to 1.0s/point), and repeats. The step increment (point spacing) is selectable at 0.25, 0.50, or 1.0μm between points. The range of the stepping motors is limited; thus the total scan length is limited to

an x-y matrix 200 x 200μm. Coarse positioning controls allowed the sample to be located with respect to the desired scan zone.

The scans for this experiment were done with a 1.0μm step increment and a total length of 200μm. In order to obtain enough data points, 10 lines of 200μm were scanned with about 0.5mm between lines. Each line was positioned with the coarse controls and the microscope was refocused. Usually there were only minor changes necessary for the refocusing; in some cases because the sample was not held planar or the sample had defects, large stage motions and large changes in objective and condenser focus were required. When this occurred the 100% transmission point was readjusted to adjust for the change in illumination. Each scan line was checked prior to scanning to avoid defects; the most common defects were emulsion pinholes and bubbles in the Estar base. These defects typically caused a considerable density shift; if required, the data reduction process could detect and eliminate such data points.

At the start of the experiment each sample was mounted on a microscope slide with mounting cement and a cover glass. These samples proved difficult to measure because the small film area tended to curl and displace the cover glass. In addition there was no assurance that the mounting medium would not change the emulsion characteristics. For these reasons, later samples were run unmounted.

They were held flat on a microscope slide with lead weights. An analysis of variance test was run to examine the effects of mounting; no effects were found; therefore, the mounted samples were treated undifferentiated from the unmounted samples.

Data Reduction

The microdensitometer data for each aperture were in the form of 10 or more lines each containing 200 data points for a sample "run." Each sample was measured using 2 square apertures, nominally 6.25 and 1.57μm on a side (measured to be an actual 6.0 ± 0.25μm and 2.0 ± 0.25μm). Since the data points were taken with a step increment of 1.0μm, there were a significant number of correlated points in each line.

These data were treated in the following process: first, the average and variance were computed for the entire set of data (2000+ points); then for each data line, sufficient points were discarded to obtain uncorrelated data points (i.e., points separated by more than the aperture width); this gave 100 data points for the 1.57μm aperture and 29 points for the 6.25μm aperture in the data line. Third, a histogram of the uncorrelated points was made for error detection; and fourth, the average and variance were calculated for each uncorrelated line.

A standard statistical test, Bartlett's Test for homogeneity of variances (Rickmers and Todd, 1967), was then

done on each line's variance to insure that each line came from the same statistical population (i.e., was representative of a particular scanned sample). If, for example, one such line failed the test (at an alpha risk of 0.05), it was discarded and the test repeated on the remaining members; 90% of the 300 sample runs met the test criteria.

After determining that each line was representative, the average variance and overall average density were calculated. The standard error for each of these statistics was also determined. The actual variance, $\sigma^2(\underline{D})$, for the total number of independent points (usually 290 for the 6.25μm aperture and 1000 for the 1.57μm aperture) was then equal to the average variance plus the standard error of the overall average density. If at this point so many lines were eliminated that the number of remaining independent points limited the confidence in the resultant $\sigma(\underline{D})$, the run was rejected and later the sample was rescanned. A flow chart of the reduction appears in Figure 13.

The run was also rejected or partitioned into separate runs (assuming enough independent data points) if the standard error on the overall average was greater than 10^{-1} times the average variance. In this way the effect of density wedging was decreased. In some cases the run was kept by deleting certain data points detected in the histogram; these were usually traced to paper tape punch errors.

The various tests applied to the data allowed determination of $\sigma(\underline{D})$ to ± 20% for any reported value. For 90% of the reported values this error is significantly lower; at a 95% confidence level, the error for $\sigma(\underline{D})_{1.57}$ is ± 5% and for $\sigma(\underline{D})_{6.25}$ is ± 10%. The homogeneity test effectively limits the largest experimental error on the determination of $\sigma(\underline{D})$ to about ± 0.002, a level of magnitude below the measured $\sigma(\underline{D})$. The criteria on the standard error of overall average density limits the experimental error on the average density to less than ± 2%.

CHAPTER 4

EXPERIMENTAL RESULTS

The Macroscopic Response

The D-Log E curves for photon and 10, 15, and 20 KEV electron exposures appear in Figures 14 and 15 for D-19 developer and in Figure 17 (p. 61) for HRP developer. The pa ameters of gamma and speed obtained from these curves appear in Table 3.

Due to the method of measuring the electron density the absolute exposure values may be in error by 10%. The relative error for exposure value is, however, on the order of 2%. The error for density values varies from point to point and is difficult to determine for some of the samples since many points plotted in Figures 14 to 17 did not meet the criteria of ± 0.02 maximum density variation used in selecting samples for granularity determination. The density value represents an average of five points in the exposed frame. Since the exposing beam is Gaussian in intensity, the frame is generally non-uniform so a linear average may be in error in relating the density to the exposure. In the worst case the maximum error appears to be on the order of ± 0.11 density units.

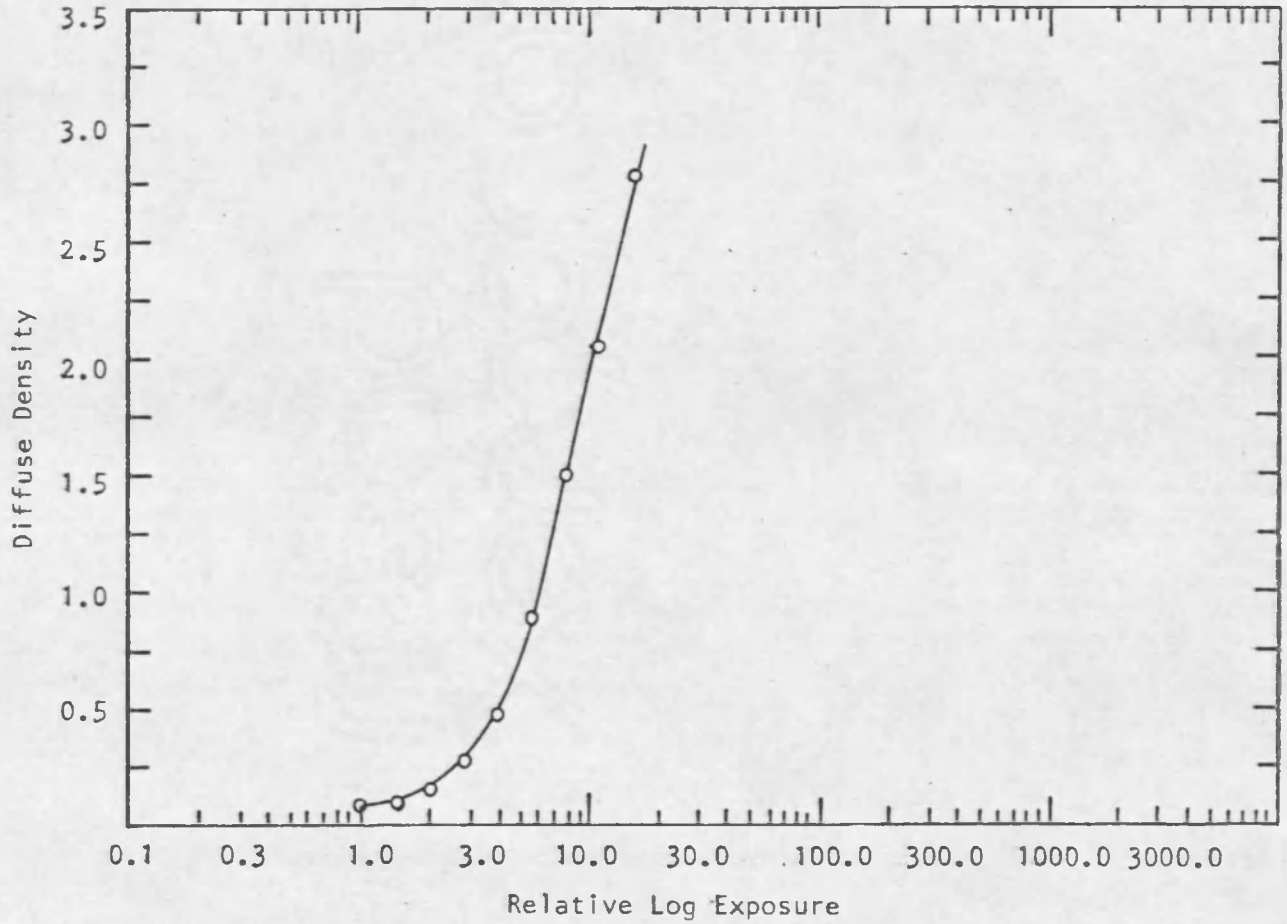

Figure 14. Photon density as a function of log relative exposure for SO-219 -- 5 min D-19, 75°F tank; Macbeth TD403, visual filter; intensity scale.

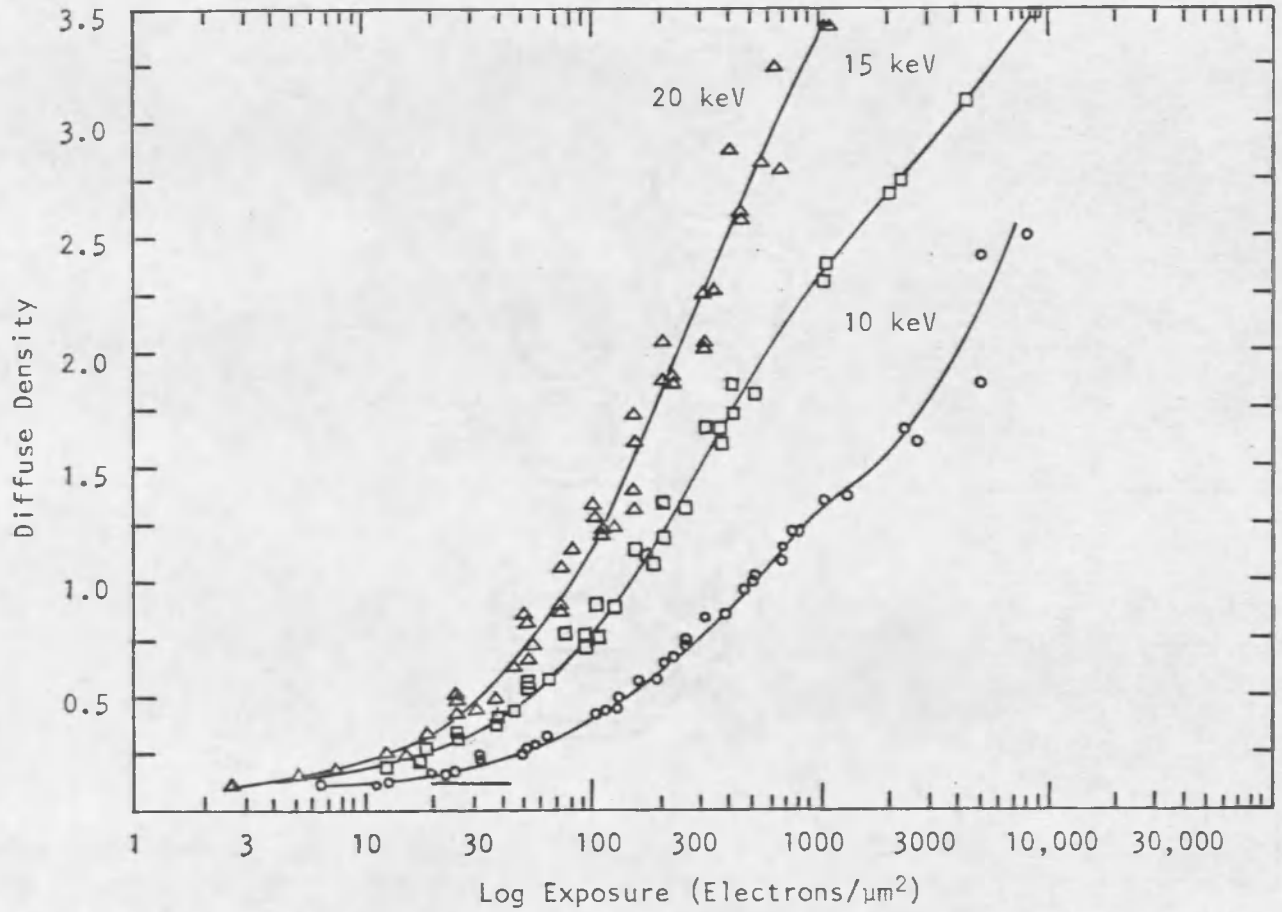

Figure 15. Electron density as a function of log exposure for SO-219 -- 5 min D-19; 75°F tank; Macbeth TD403, visual filter; time scale; intensities between 5 and 200 pA/cm^2.

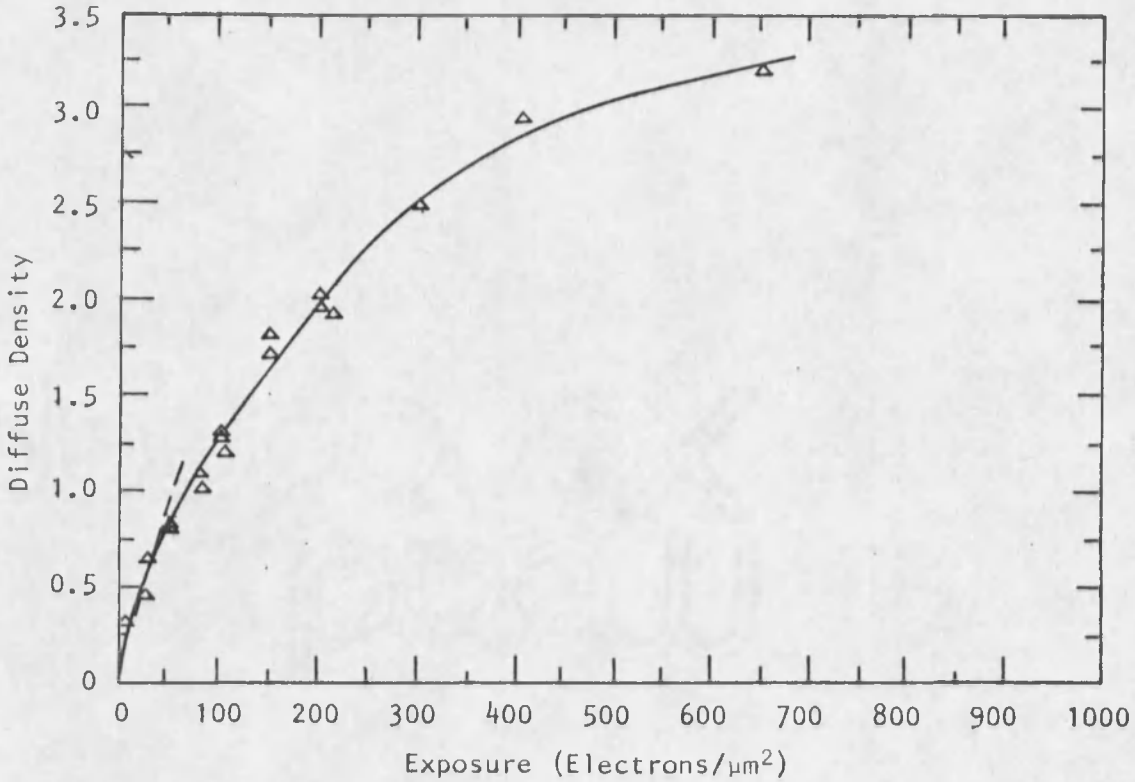

Figure 16. 20 KEV electron density as a function of exposure -- 5 min D-19, 75°F tank; Macbeth TD403, visual filter; low intensity beam 30 to 40 pA/cm^2.

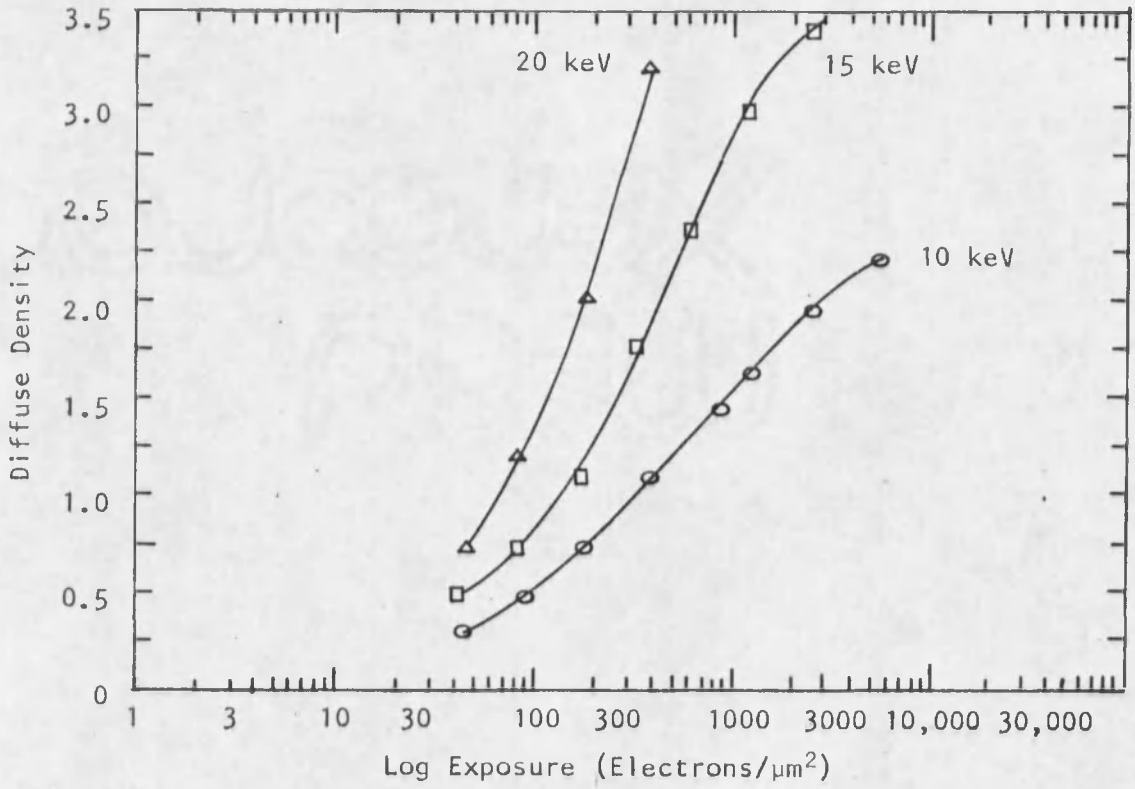

Figure 17. Electron density as a function of log exposure -- HRP (1:4) plus 5 gm/liter benzotriazole; 12 min, 75°F tank; Macbeth TD403, visual filter; time scale; intensity 700 pA/cm^2.

Table 3. D-log E curve parameters.

Exposing energy	Gamma (slope)	Speed at D = 1.08	
		$\frac{1}{E}$ $e^-/\mu m^2$	$\frac{1}{E}$ $\mu m^2/e^-$
	D-19 developer		
Photon	4.16		
20KEV	2.37	96	0.0105
15KEV	1.68	175	0.00571
10KEV	1.21	670	0.00149
	HRP developer		
20KEV	3.69	85	0.0117
15KEV	1.94	165	0.00606
10KEV	1.10	420	0.00238

Another factor accounting for the data scatter is that Figure 15 was obtained from several intensity levels and several exposure runs. The curves in Figure 18 were obtained by exposing one roll of film to two different intensity levels at each acceleration voltage. These latter curves, then, are not from separate runs and since the development was the same for each curve, they do not have this run-to-run variability.

The shift in exposure for the 15 and 20 KEV electron exposures are presented in Table 4. Since this shift is greater than the expected variability in exposure, there is evidence of reciprocity failure for these accelerations. The 10 KEV exposure does not exhibit a shift over the density range tested. At higher densities a shift may be possible and could explain the odd behavior of the 10 KEV curve in Figure 15; the exposures necessary to obtain a density near 2.5 were very much longer (one and two hours exposure time) than the typical few minutes. Over the longer time significant fluctuations in electron density are probable.

Due to problems in temperature control the development temperature varied from run to run. Table 5 presents the extent of this variability; the curves for the two temperature extremes, 72 and 76 degrees F, appear in Figure 19. The 10 KEV exposure was chosen since it should show the

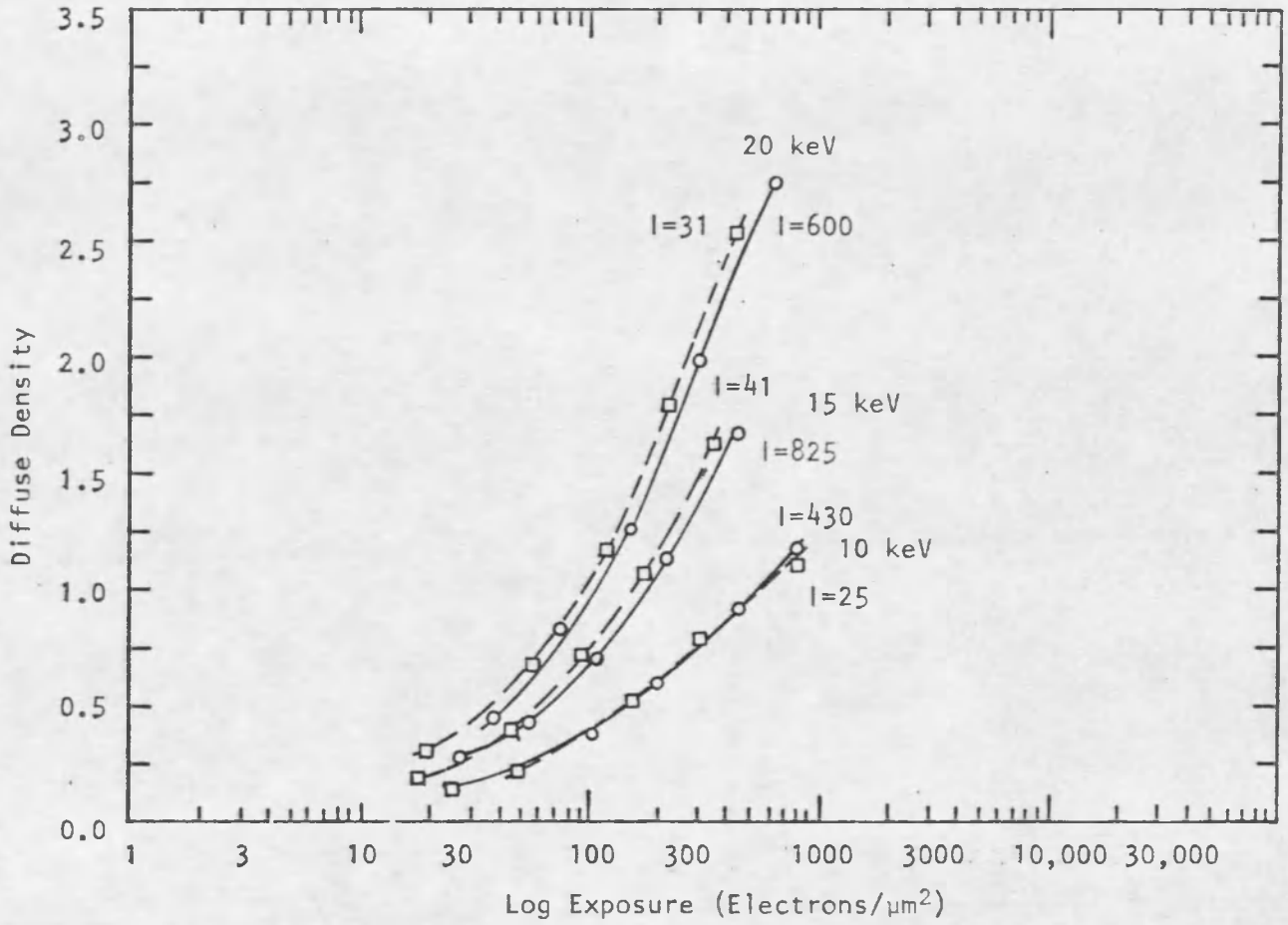

Figure 18. Electron density as a function of log exposure for high intensity (solid lines) and low intensity (dashed lines) -- D-19, 5 min, 75°F tank; Macbeth TD403, visual filter; intensities (I) in pA/cm^2.

Table 4. Reciprocity parameters.

Density	Exposing energy					
	20KEV			15KEV		
	E_H	E_L	E_H/E_L	E_H	E_L	E_H/E_L
0.5	43	36	1.20	64	58	1.10
1.0	110	95	1.16	181	155	1.17
1.5	192	172	1.12	360	300	1.20
2.0	320	275	1.16			
2.5	500	440	1.14			

E_H = High intensity exposure ($e^-/\mu m^2$).

E_L = Low intensity exposure ($e^-/\mu m^2$).

Table 5. Development temperature variability.

Run number	Temperature °F
6	72
7	76
8	72
9	76
10	75
11	75
Photon	75

All D-19, 5 min tank except runs 8 and 11. Run 8 tray development for development series. Run 11, HRP, 12 min tank.

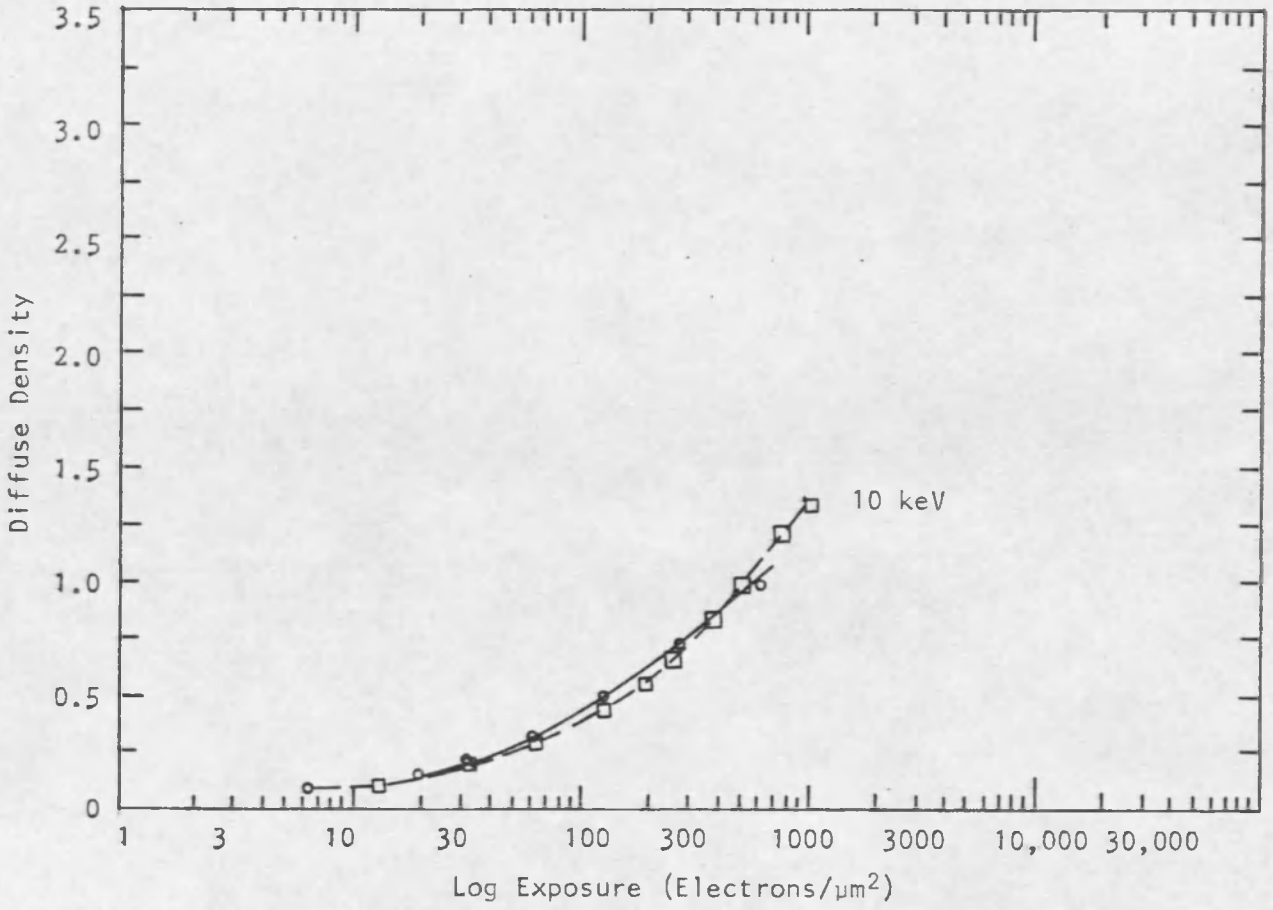

Figure 19. Electron density as a function of log exposure for 75°F (solid line) and 72°F (dashed line) -- D-19, 5 min, 75°F tank; Macbeth TD403, visual filter; intensity 103 pA/cm^2; time series.

largest developmental effect. No significant effect due to temperature variability was detected.

The effect of development time variations is shown in Figure 20. The curves passed through each point have been obtained by shifting the curve for the 20 KEV exposure along the Log E axis in order to extrapolate to a common density. Although theory predicts that the curve shape should not change, this procedure may not be correct. The speed ratios appear in Table 6. These speed ratios, evaluated at a density of one, are not proportional to the ratio of the densities at the common exposure point. This indicates that the D-E curve is non-linear.

Figure 16 illustrates the extent of the non-linearity for 20 KEV electrons. Since the range of a 20 KEV electron is greater than that of a 10 or 15 KEV electron, this response curve should show the least departure from linearity. This is also visible in Figure 15; a consequence of a linear D-E curve is a progressively steeper D-Log E curve (the slope should increase as 2.3D). The 20 KEV curve comes closest to this ideal. In addition, the maximum density for the 20 KEV exposures was greater than 4.5, hence contributing to linearity. The observed non-linearity suggests that the one hit exposure process does not apply.

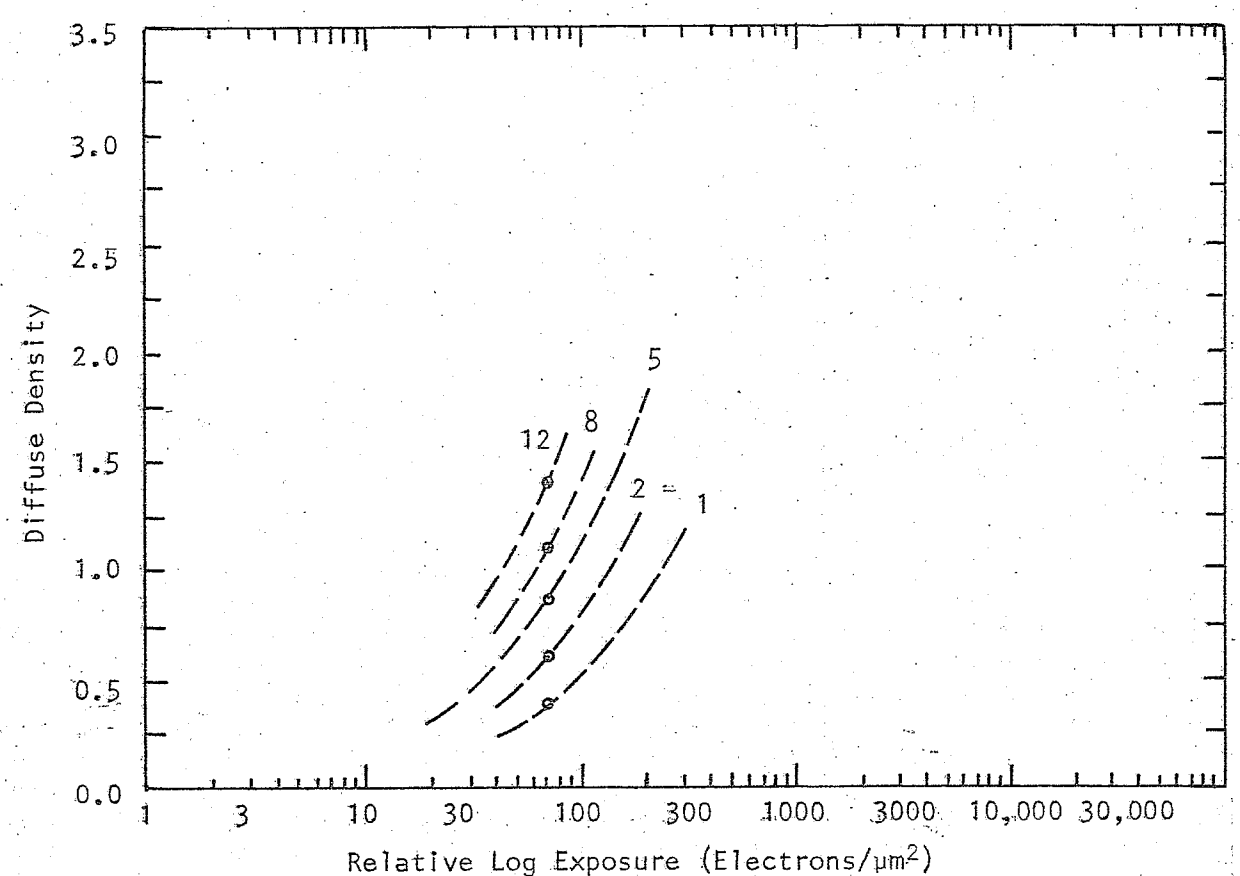

Figure 20. Electron density as a function of log exposures for five development times (in minutes) -- D-19, 72°F tray; Macbeth TD403, visual filter. Data point is for a common exposure. Curves are extrapolated from 5 min curve.

Table 6. D-19 development series.

Development time (min)	Relative exposure ($e^-/\mu m^2$)	Speed ratio	Base plus fog density
1	240	0.33	.05
2	140	0.57	.05
5	88	1.00	.08
8	62	1.29	.09
12	44	1.81	.20

Granularity

Photomicrographs of representative samples used for the granularity measurements appear in Figures 21 to 24. These samples have a density close to one and illustrate the uniformity of exposure.

Curves illustrating the variation of Log$\sigma(\underline{D})$ with Log $(\overline{\underline{D}})$ appear in Figure 25. The points on these curves have (at 95% condidence) errors of ±5% for the small scanning aperture and ±10% for the larger. The electron exposed emulsions show a rise of $\sigma(\underline{D})$ with $\underline{D}$ to about a density of one; the value of $\sigma(\underline{D})$ then begins to decrease. The location of the maximum appears to increase with acceleration potential. Photon exposures have a slower rise of $\sigma(\underline{D})$ with increasing $\underline{D}$ up to a density of one; at higher densities $\sigma(\underline{D})$ increases more rapidly with $\underline{D}$.

A least squares analysis was used to fit the data to a function of the form:

$$\sigma(D) = A\ \overline{D}^{B}, \qquad (32)$$

The value of the parameter $\underline{A}$ represents the square root of 0.434 times the mean grain size to aperture size ratio, and the parameter $\underline{B}$ should be 0.5 for the theory previously discussed. Values of $\underline{B}$ between 0.3 and 0.5 have been reported by previous investigators.

Table 7 lists the derived values for the two parameters and the correlation coefficient for the equation and

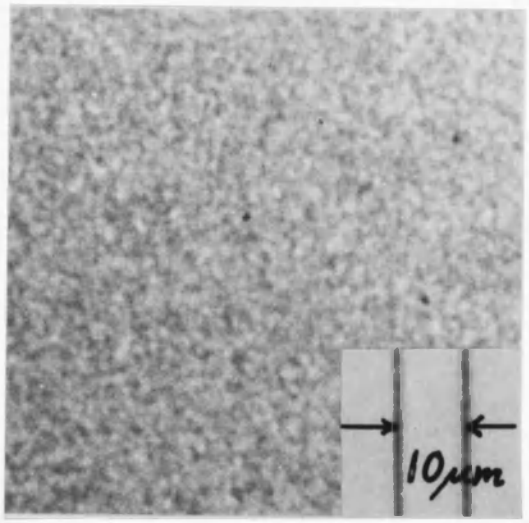

Figure 21. Photon exposure.

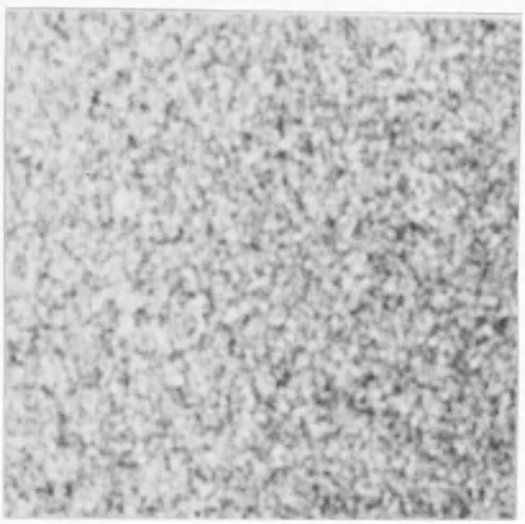

Figure 22. 10 KEV exposure.

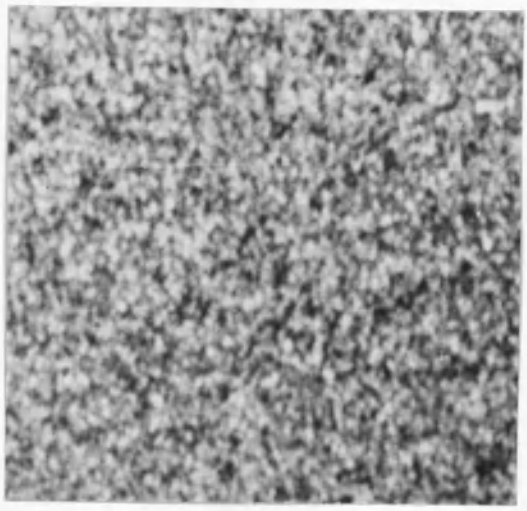

Figure 23. 15 KEV exposure.

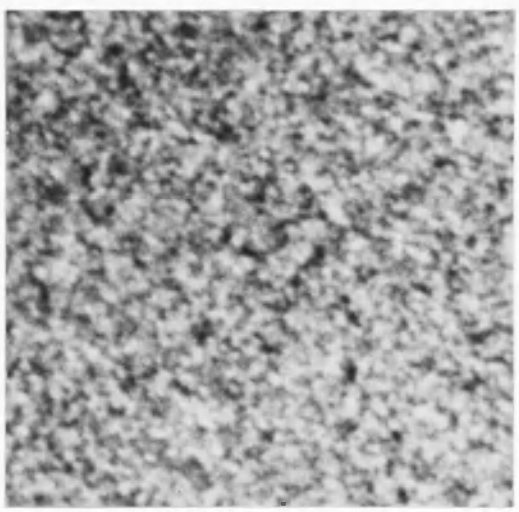

Figure 24. 20 KEV exposure.

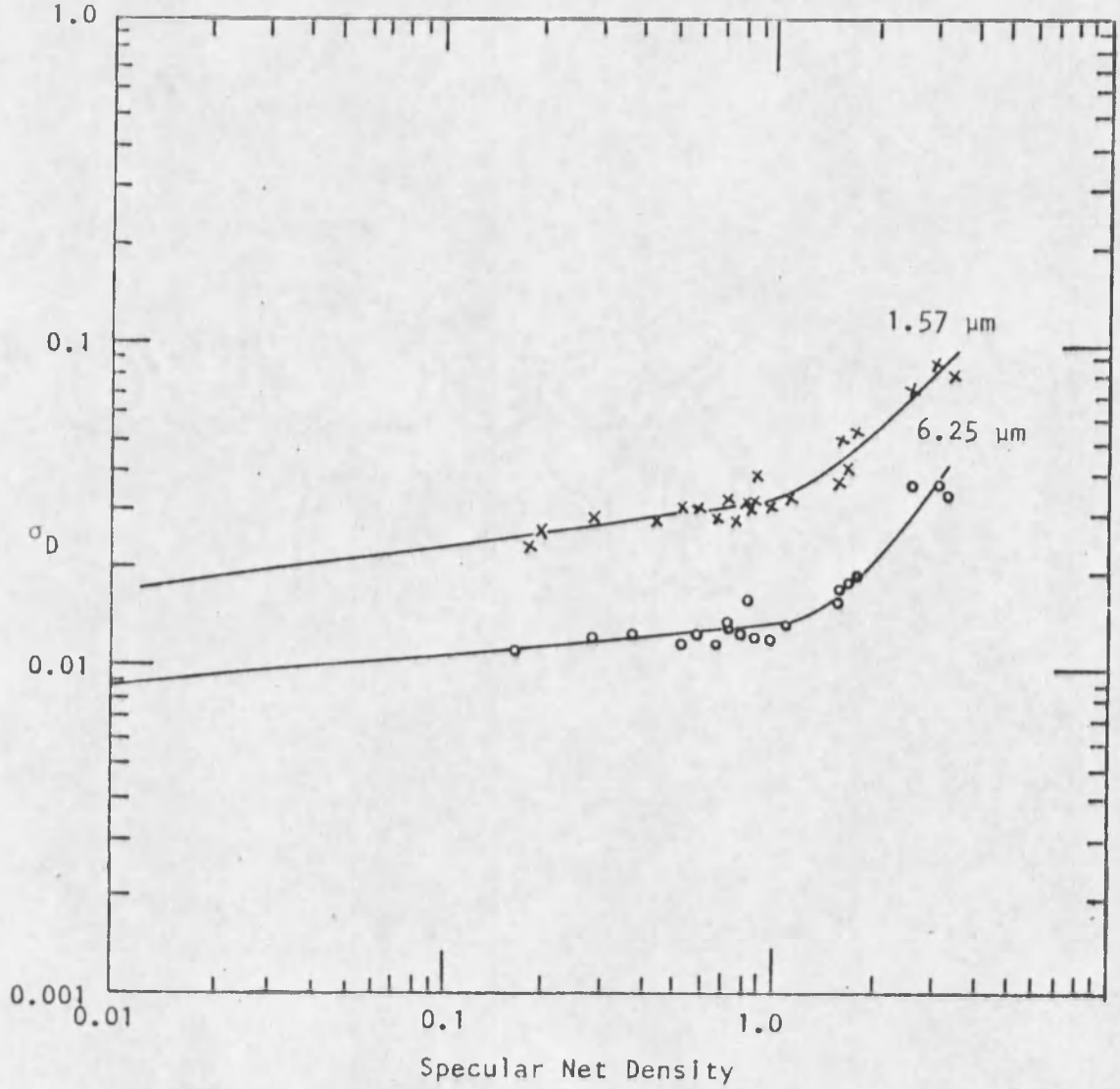

(a) Photon exposure. x = 1.57 µm aperture, o = 6.25 µm aperture. D-19 developer, 5 min, 75°F tank.

Figure 25. Variation of Log σ_D and Log D.

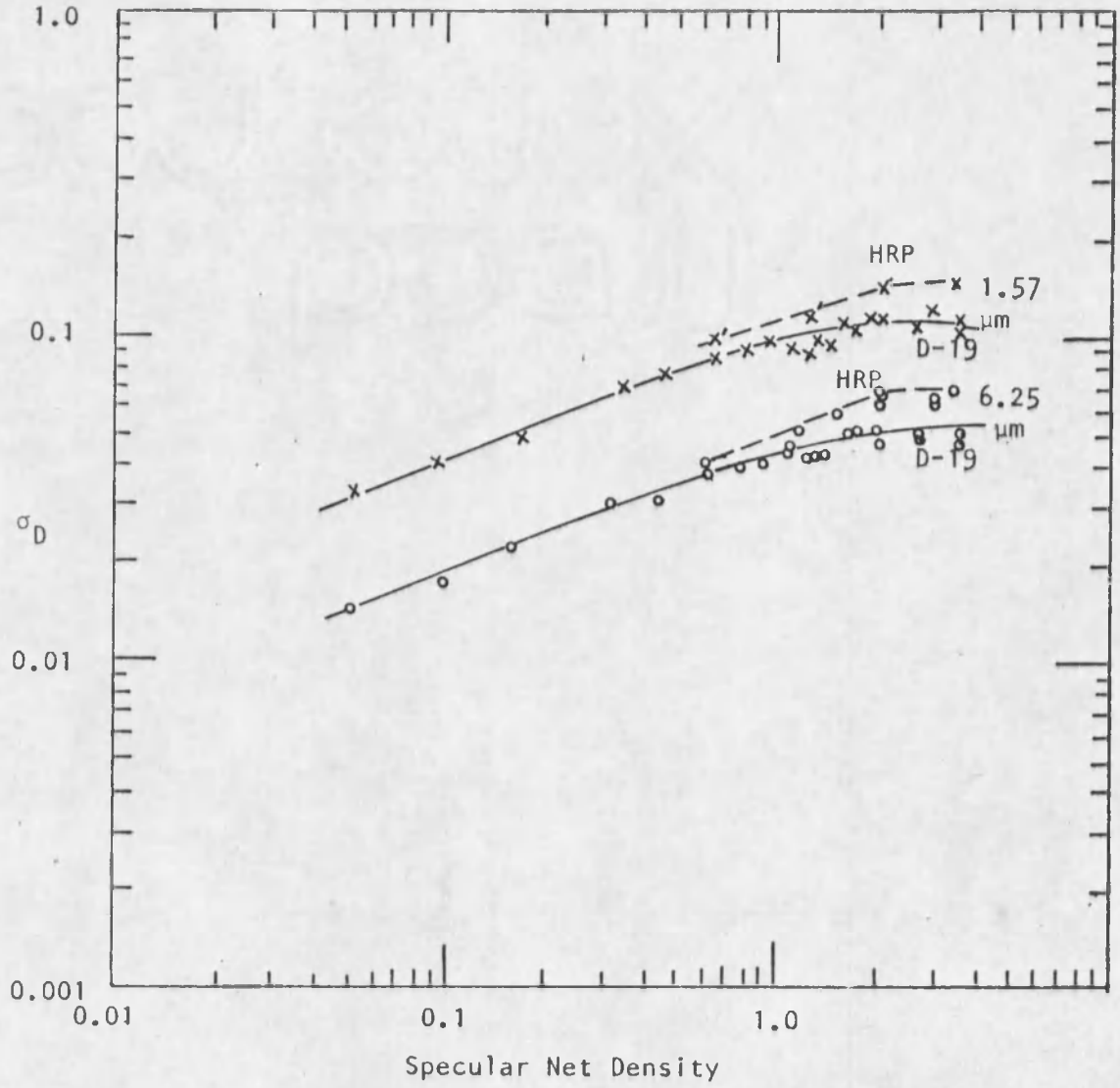

(b) 20 KEV electron exposure. x = 1.57 μm aperture; o = 6.25 μm aperture; x,o = D-19 developer, 5 min, 75°F tank; x',o' = 12 min, 75°F tank.

Figure 25.--Continued Variation of Log σ_D and Log D.

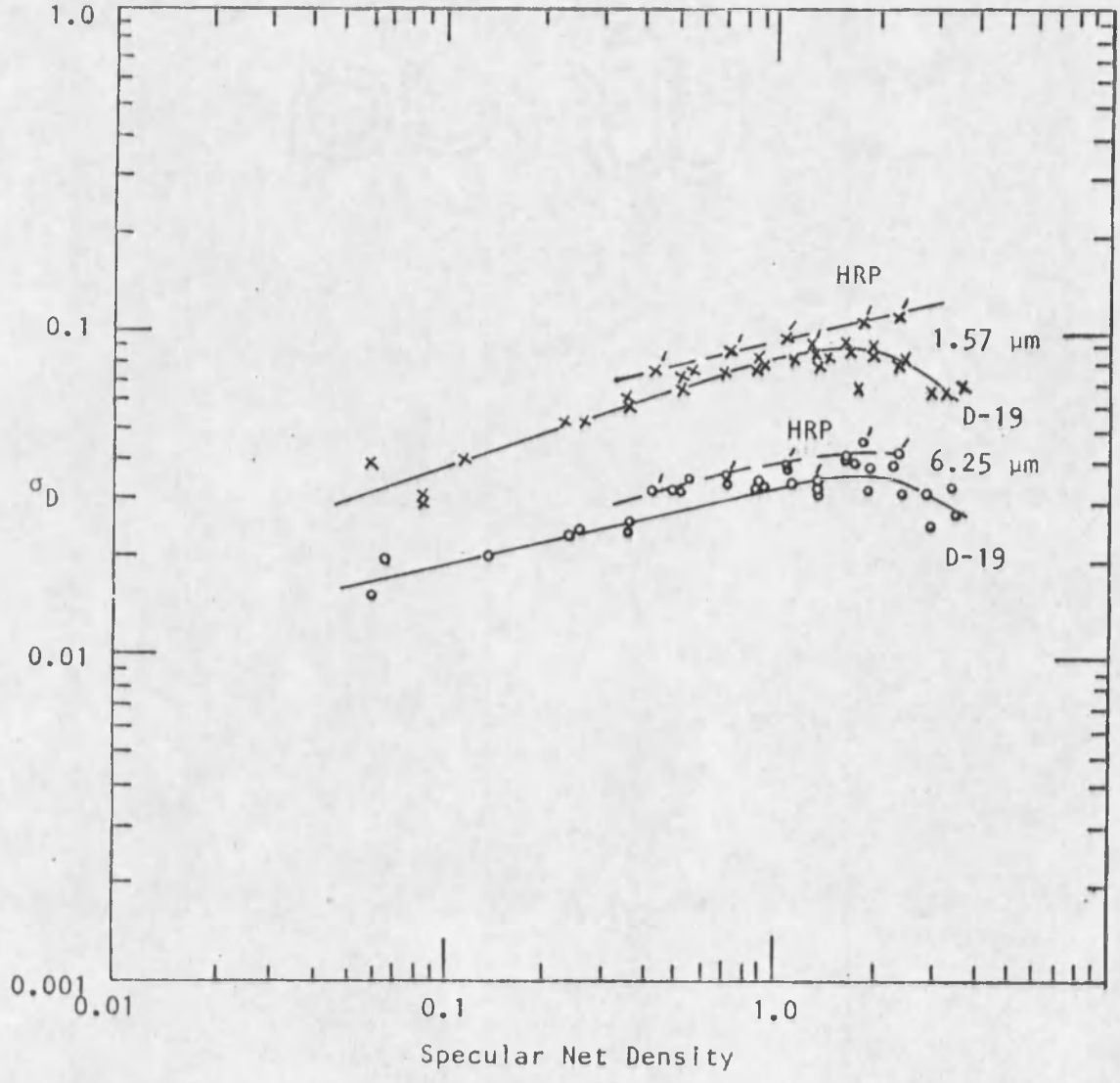

(c) 15 KEV electron exposure. x',x = 1.57 µm aperture; o',o = 6.25 µm aperture; x',o' = HRP developer, 12 min, 75°F tank; x,o = D-19 developer, 5 min, 75°F tank.

Figure 25.--Continued Variation of Log σ_D and Log D.

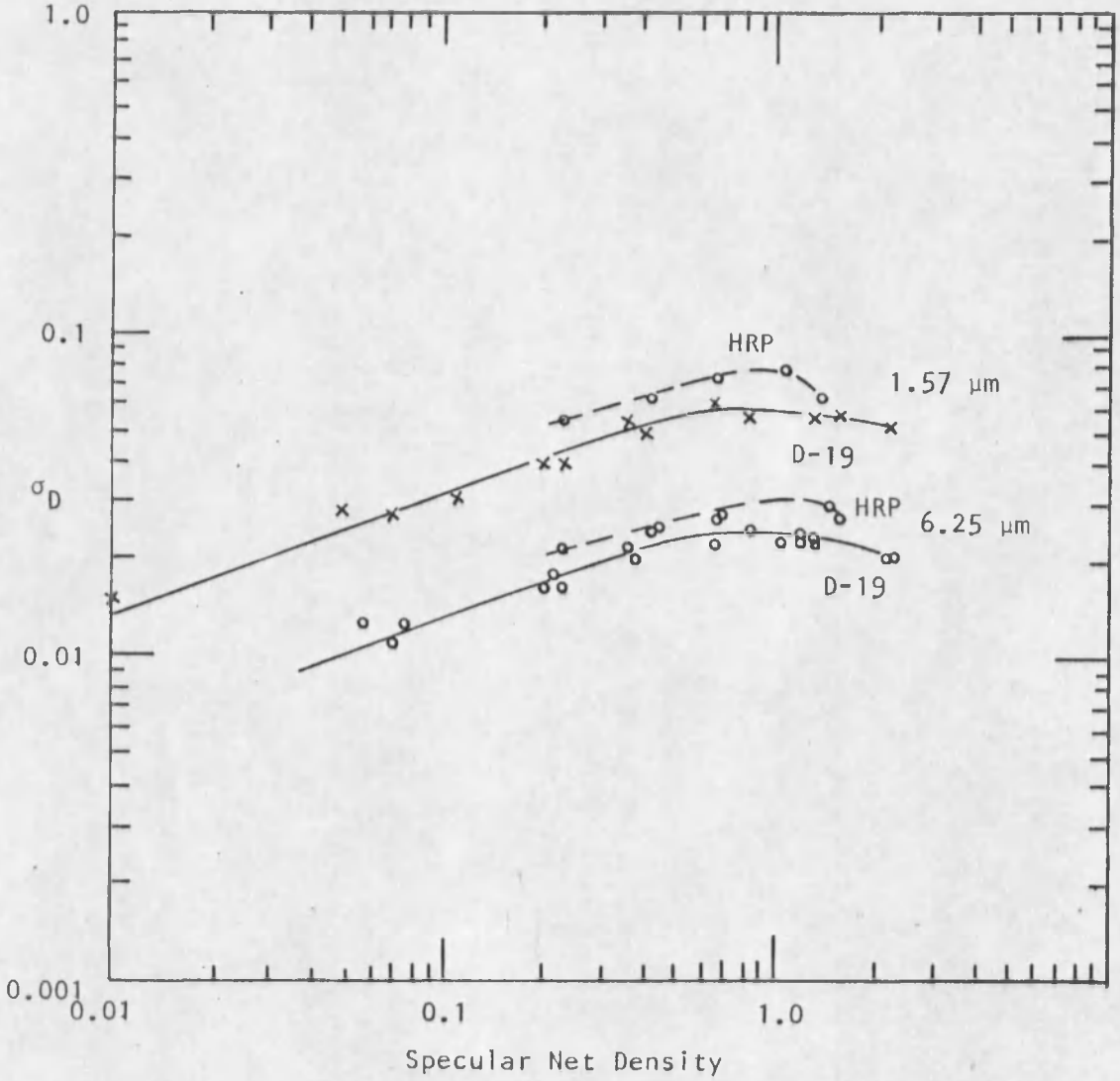

(d) 10 KEV electron exposure. x,x' = 1.57 μm aperture; o,o' = 6.25 μm aperture; o',x' = HRP developer, 12 min, 75°F tank; o,x = D-19 developer, 5 min, 75°F tank.

Figure 25.--Continued Variation of Log σ_D and Log D.

Table 7. Least square fit of the relation $\sigma(D) = AD^B$.

Exposing energy	Aperture (μm)	Density to	Correlation Coefficient and (number of points)	B	A	Ratio A1.57/A6.25
Photon	6.25	3.2	0.73 (20)	0.23	0.017	
		0.95	0.78 (12)	0.086	0.013	
		>0.95	0.96 (8)	1.00	0.012	
	1.57	3.2	0.52 (23)	0.26	0.045	2.68
		0.95	0.30 (15)	0.18	0.041	3.04
		>0.95	0.98 (8)	0.81	0.034	2.88
20 KEV	6.25	0.94	0.99 (9)	0.37	0.043	
		1.7	0.98 (17)	0.37	0.043	
		3.5	0.95 (25)	0.32	0.041	
	1.57	0.95	0.99 (9)	0.37	0.100	2.34
		1.9	0.98 (18)	0.33	0.094	2.16
		3.5	0.95 (25)	0.29	0.089	2.17
15 KEV	6.25	0.91	0.95 (13)	0.28	0.035	
		2.0	0.92 (23)	0.23	0.032	
		3.5	0.76 (28)	0.16	0.030	
	1.57	1.1	0.98 (14)	0.36	0.084	2.57
		1.7	0.97 (21)	0.31	0.078	2.46
		3.5	0.81 (29)	0.21	0.070	2.33

Table 7.--Continued

Exposing energy	Aperture (μm)	Density to	Correlation Coefficient and (number of points)	B	A	Ratio A1.57/A6.25
10 KEV	6.25	0.88	0.78 (13)	0.19	0.025	
		1.6	0.82 (19)	0.17	0.024	
		2.5	0.78 (21)	0.15	0.023	
	1.57	0.67	0.78 (9)	0.31	0.061	2.44
		1.2	0.85 (12)	0.28	0.058	2.41
		2.5	0.84 (16)	0.22	0.052	2.29

data. The data points from electron exposures were analyzed sequentially, taking the lower portion of the curve first (below a density of one). Except for the 10 KEV exposures, excellent correlation was obtained up to the maximum value for $\sigma(\underline{D})$ with values for $\underline{B}$ between 0.23 and 0.37; beyond this maximum, where the curve slope for $\underline{\sigma(D) - (D)}$ changes sign, the correlation, as expected, was lower (0.7) and the parameter $\underline{B}$ then ranges from 0.16 to 0.32.

For 10 KEV exposures the correlation is weaker than for 15 or 20 KEV exposures, but is nevertheless still greater than 0.7. Values of $\underline{B}$ seemed to be more aperture dependent (lower for the larger aperture) than expected.

For photon exposures the situation was quite different. The relationship between $\sigma(\underline{D})$ and $\underline{D}$ was tested in the region 0.0 to 0.95 density and 0.95 to 3.2 density. The second region had a higher correlation to the test equation but returned values for $\underline{B}$ between 0.81 and 1.0. The lower region had a weaker correlation (0.78) and resulted in values for $\underline{B}$ between 0.086 and 0.18.

The low values for $\underline{B}$ tend to indicate that the theoretical model used does not account for the data. This effect may be associated with the extremely fine grain of the tested emulsion; the individual grains were difficult to resolve during focusing of the microdensitometer. For such small grains there may be considerable scattering of the measuring light; this was not considered in arriving at

the theoretical model so it may not be surprising that B was not 0.5.

The ratio of values of the parameter A for the two apertures is a direct measure of aperture "diameter" since for the model used:

$$A = [(0.434)(a'/a)]^{1/2} \tag{33}$$

with a', the mean grain area, and a the projected aperture area; therefore:

$$A_{1.57}/A_{6.25} = (a_{6.25}/a_{157})^{1/2}. \tag{34}$$

This ratio varied between 3.04 and 2.16 and was generally lower for the electron exposed emulsions. The average value of 2.48 should then represent the ratio of the square aperture widths. Using the nominal aperture sizes, the ratio should be about 3.9.

The aperture sizes were experimentally determined by scanning a knife edge (razor blade). The distance between the zero and 100% transmission points was taken as the aperture width. These values were 2.0 ± 0.25μm and 6.0 ± 0.25μm for the two apertures. This gives an aperture ratio of 3.0 ± 0.5.

The ratio for photon exposure was within the tolerance for the measured aperture ratio. For electron exposed emulsions the calculated ratio appears lower than expected. This may be caused by a grain aggregate size

approaching the aperture dimensions which would invalidate the assumptions used to derive the theoretical model.

Visible differences can be observed between the sample photomicrographs in Figures 21 to 24. All were photographed and processed identically and all have a macro density of one. The 10 KEV exposure is more nearly comparable in appearance to the photon exposure than either of the other two samples. This 10 KEV exposure, nevertheless, shows the "clumpy" consistency of electron exposure which is visible in the 15 and 20 KEV exposures. Aggregation does take place.

Referring again to Figure 25, the curve shapes (Log $\sigma(\underline{D})$ - Log $(\underline{D})$) for HRP developed emulsions are similar over their density ranges to the D-19 developed emulsions. The increase in $\sigma(\underline{D})_{HRP}$ is compensated in part by an increase in speed. With higher speed, fewer electrons are required to produce a given density, hence the input quanta noise increases. For 20 KEV electrons $\sigma(\underline{D})_{HRP}$ increases by about 15% while speed increases by 25%. This causes a decrease, however, in the number of detectable density levels or DDL's (Eyer, 1962).

These levels, defined at intervals of $\pm 5\ \sigma(\underline{D})$, are tabulated in Table 8. They represent a measure of recording capacity. The HRP developed emulsions have fewer levels than the D-19 processed emulsions; this may not be compensated by the gain in speed.

Table 8. Detectable density levels (DDL).

Exposing energy	Developer	Number of DDL	Density range	Speed
10 KEV	HRP	7	2.3	420
15 KEV	HRP	6	3.1	165
20 KEV	HRP	4	3.3	85
Photon	D-19	15	3.0	--
10 KEV	D-19	9	2.0	670
15 KEV	D-19	11	3.5	175
20 KEV	D-19	7	3.5	96

Note: DDL's defined at $\pm$ 5 σ_D intervals using a 6.25 µm aperture. Speed calculated in electrons/sq µm to reach a net D = 1.0.

There may be a more optimum development time for the maximum number of DDL's for D-19. A time series was run to examine this; these data appear in Figure 26. The curves were obtained from Figure 25 and were used to compute Table 9, the change in $\sigma(\underline{D})$ with development time. With the shorter time there was a loss in speed and $\underline{D}_{MAX}$ and these losses make the decrease in $\sigma(\underline{D})$ less useful in increasing the DDL's. There was one time, other than the standard 5 minutes, which appears to have advantages. An 8 minute development resulted in an increase in $\sigma(\underline{D})$ of about 2% and an increase in speed of about 30%. Although $\underline{D}_{MAX}$ was not measured, it is expected to be higher for the longer time,

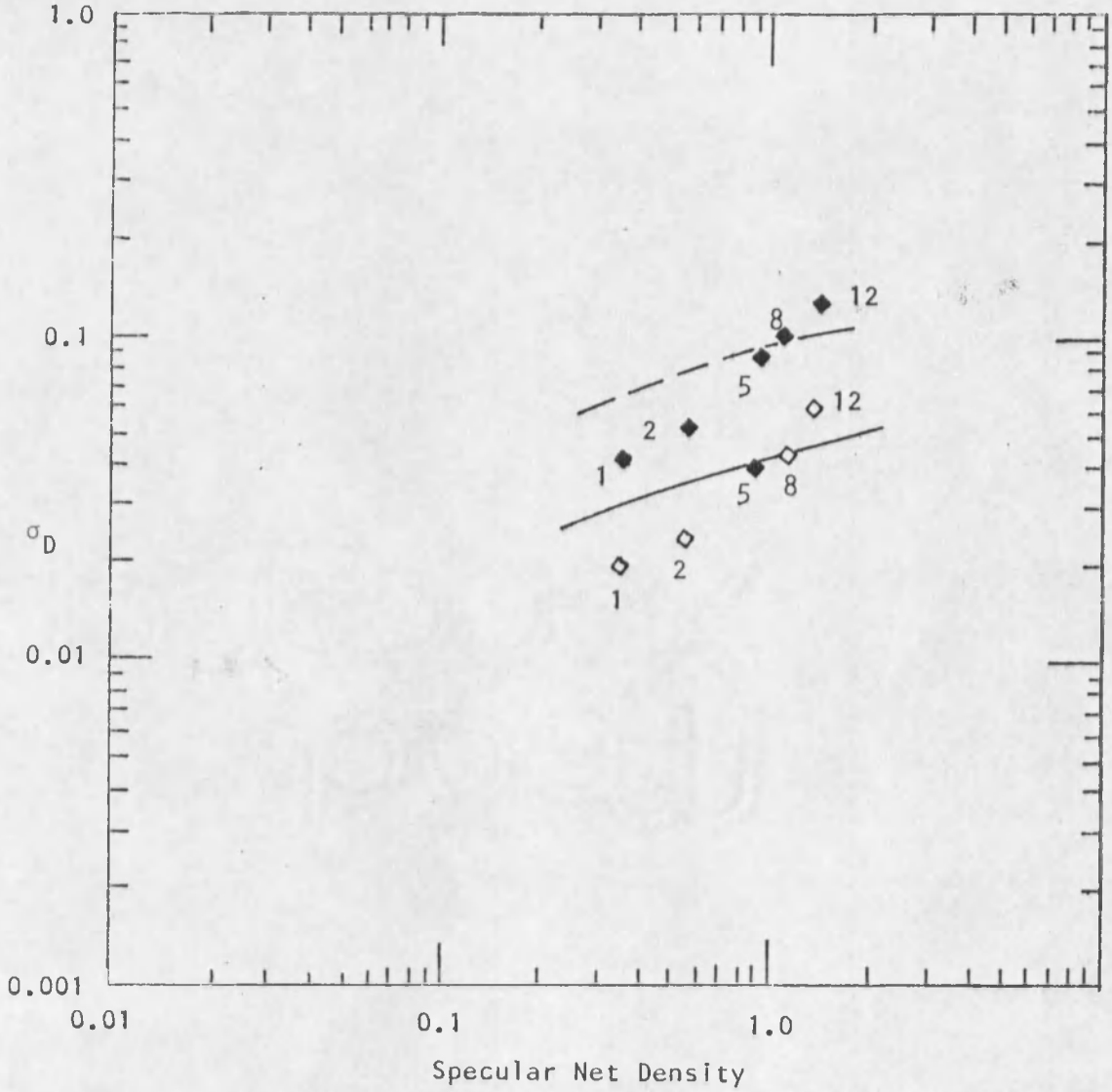

Figure 26. Development time variations in σ_D for 20 KEV electron exposure -- D-19, 75°F tank. ◆ = 1.57 μm aperture, ◇ = 6.25 μm aperture. Curves are for σ_D-D at 5 min.

Table 9. Change in granularity for various development time -- D-19, 72°F tank, 20 KEV electrons.

Time t (min)	$\sigma(D)$ (6.25 μm)	Speed ratio (at D = 1)	$\frac{\sigma(D_t)_t}{\sigma(D_t)_{5\ min}}$	D_t
1	0.0195	0.33	0.65	0.33
2	0.024	0.57	0.67	0.52
5	0.040	1.00	1.00	0.85
8	0.045	1.29	1.02	1.08
12	0.063	1.81	1.40	1.32

thus increasing the number of DDL's. The 8 minute time appears more optimum than the standard 5 minutes.

Figure 27 shows the run-to-run variability in computing the granularity coefficient, $\sigma(\underline{D})(2\underline{a}/\underline{D})^{1/2}$, by run number for 15 KEV electrons. The conditions of exposure and processing do not seem to introduce large errors; Table 6 gives the development conditions for the runs.

The curves of Log $\sigma(\underline{D})(2\underline{a}/\underline{D})^{1/2}$ - Log $\underline{D}$ appear in Figure 28. These curves have an estimated precision of ±15% considering all the errors (±10% on $\sigma(\underline{D})$, ±3% on the aperture area, $\underline{a}$, and ±2% on $\underline{D}$). In the simple model used here, the Selwyn granularity $\underline{G} = (2\underline{a})^{1/2}\sigma(\underline{D})$, the factor $\sigma(\underline{D})(2\underline{a}/\underline{D})^{1/2}$ should express the mean grain area, $\underline{a}'$, and this should remain constant. The decrease in $\sigma(\underline{D})(2\underline{a}/\underline{D})^{1/2}$ with $\underline{D}$, exhibited in Figure 28, then implies a decreasing grain size. Again the radical difference between photon and electron exposure after a density of one is observable. Up to a density of one the photon exposure shows the largest rate of decreasing mean grain size, while for electron exposure the largest rate occurs for 10 KEV electrons. Above a density of one, the electron exposures show a faster decrease in grain size than for the lower densities. This may be explained by reasoning that, as the grain aggregates become closer and closer (nearing the maximum density), then the density fluctuations due to these aggregates begin to decrease while the fluctuations due to the grains

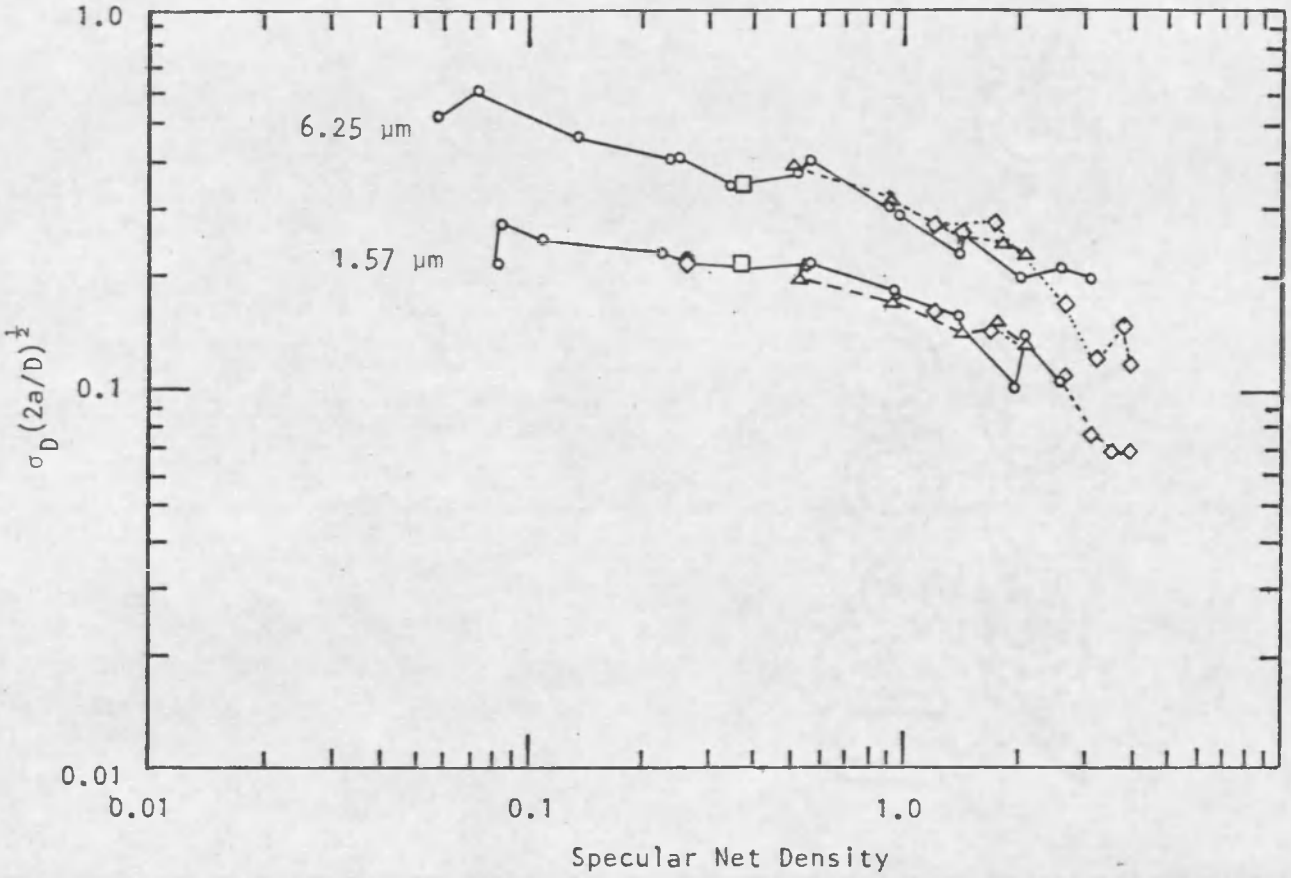

Figure 27. Run-to-run variability for 15 KEV electron exposure -- Δ = run 6, o = run 7, ◇ = run 9, □ = run 10.

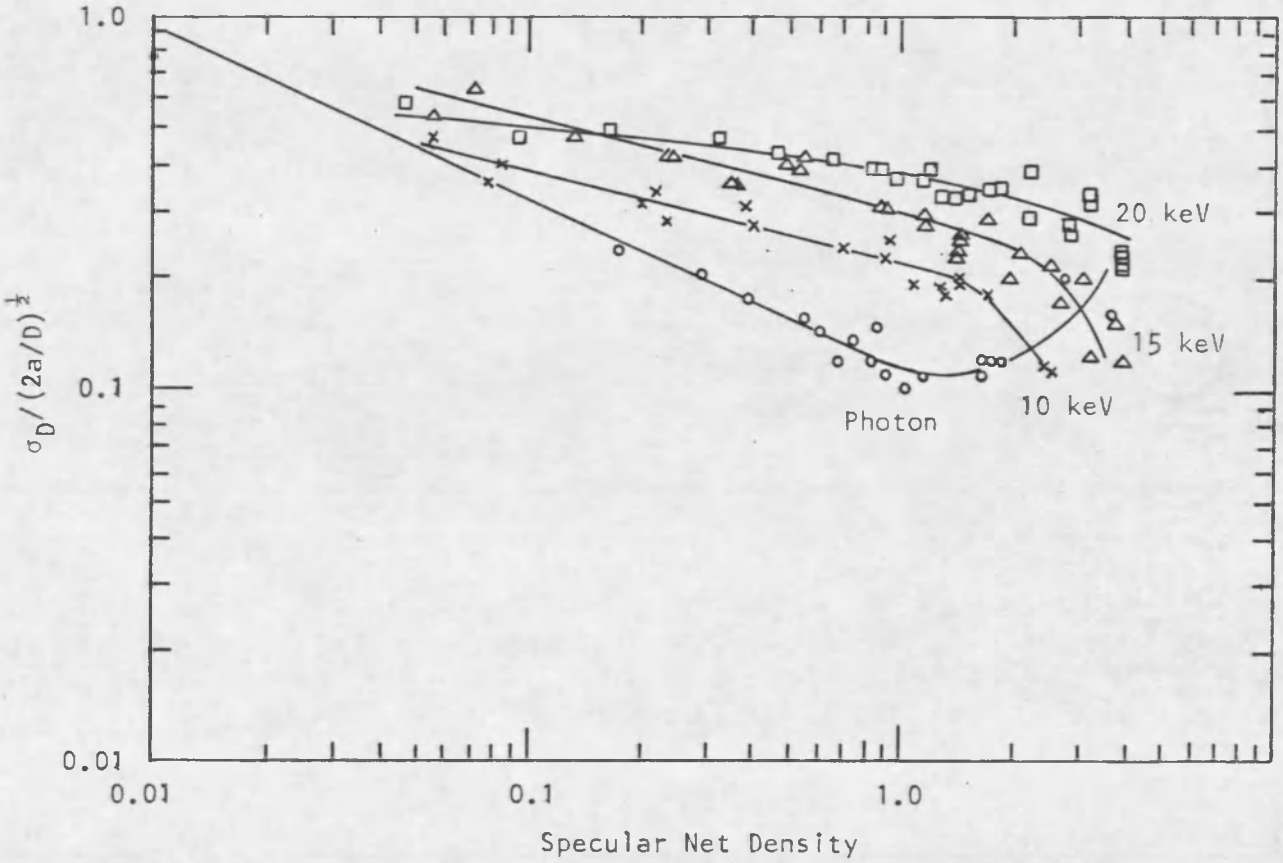

(a) 6.25 μm aperture; D-19. ○ = photon, □ = 20 KEV, Δ = 15 KEV, x = 10 KEV.

Figure 28. Granularity as a function of specular net density.

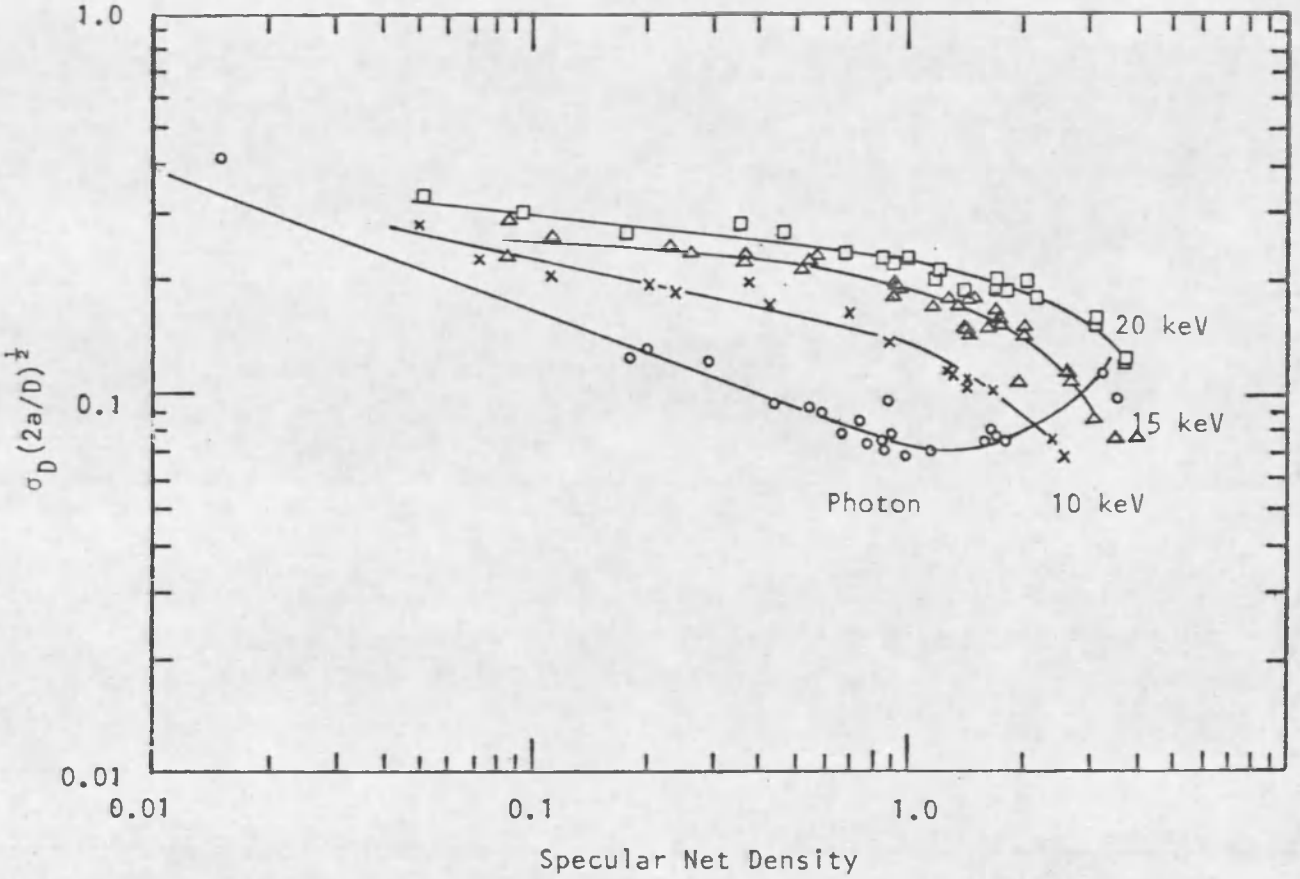

(b) 1.57 μm aperture; D-19. o = photon, □ = 20 KEV, Δ= 15 KEV, x = 10 KEV.

Figure 28.--Continued Granularity as a function of specular net density.

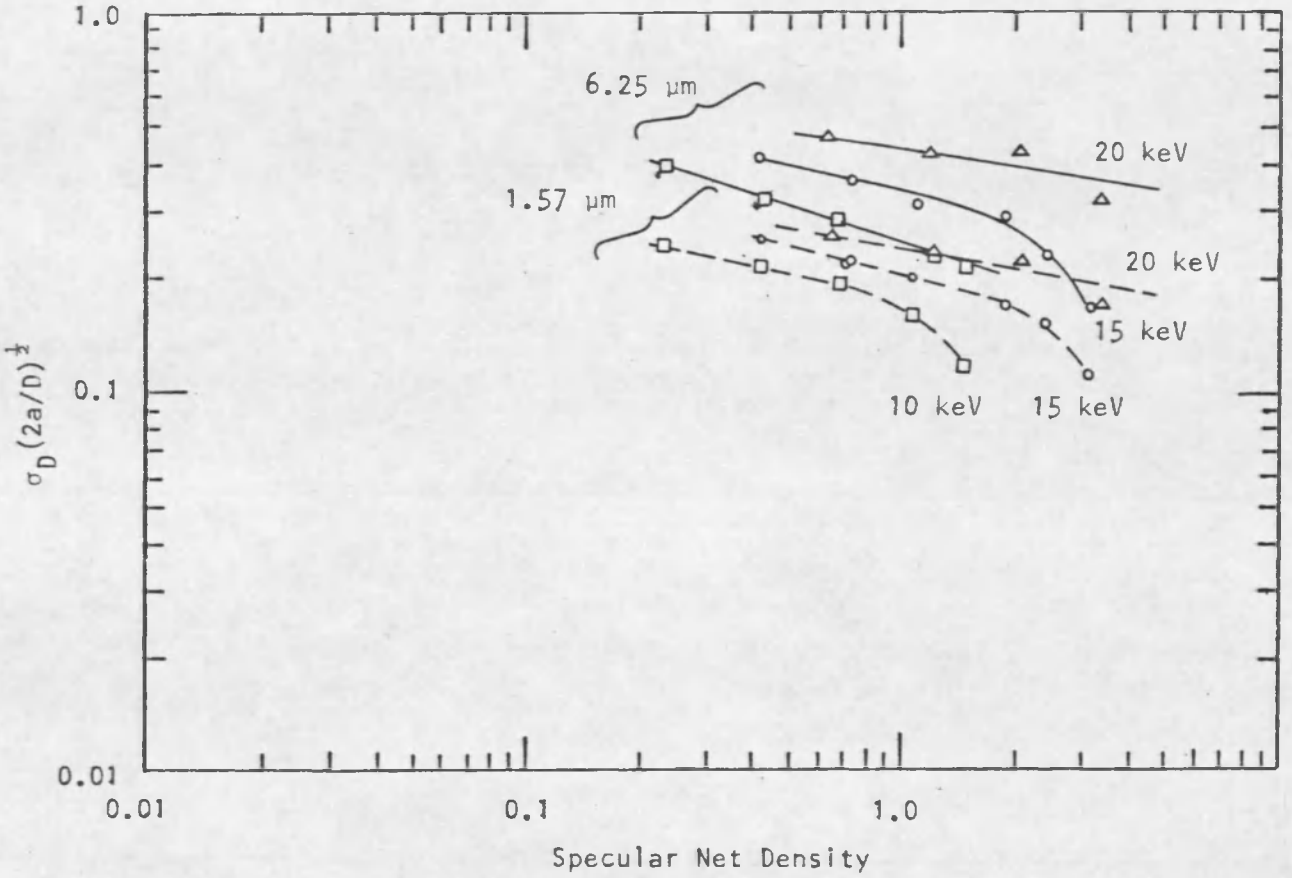

(c) HRP, 12 min, 75°F tank. Δ = 20 KEV, o = 15 KEV, □ = 10 KEV.

Figure 28,--Continued Granularity as a function of specular net density.

themselves become relatively constant. The tail of the 20 KEV curve very nearly matches the slope of the photon exposure at a density less than one, indicating perhaps the variation in primary mean grain size. The other electron exposure curves do not match nearly as well, due most probably to the limitation of a lower maximum density.

The rise in the photon exposure curve above a density of one may be explained by Bayer's (1964) results which predict an increase in $(\underline{D})$ with $\underline{D}$ at higher densities due to the change in transmission by overlapping grains. The actual increase was less than he predicted for typical values of $\underline{a}$ and a'; however, the presence of scattered light tends to lower the curve.

Table 10 lists the curve derived values for $\sigma(\underline{D})$, $\sigma(D)(2\underline{a}/\underline{D})^{1/2}$, and $\underline{a}'$, grain area, for D-19 developer; the same parameters appear in Table 11 for HRP developer. The HRP grainssizes appear to be about 30% greater than the D-19 grain sizes. The grain sizes calculated for photon exposures appear to have mean radii on the order of, or less than, the optical resolution limit. In this case the use of the simple model is probably questionable.

Comparison With Other Investigators

Valentine's (1966) relation between $\sigma(\underline{D})$ and the input noise is:

$$\frac{\sigma(D)}{D} = \frac{1}{(M)^{1/2}} \quad (1+2/Q)^{1/2}, \qquad (35)$$

Table 10. Curve derived granularity values (D-19) -- D-19 developer, 6.25 μm aperture.

Density	Photon	20 KEV	15 KEV	10 KEV
		Exposing energy		
		$\sigma(D)$		
0.5	0.0130	0.035	0.0265	0.0225
1.0	0.0139	0.043	0.032	0.0235
1.5	0.0162	0.048	0.035	0.0230
2.0	0.0222	0.052	0.035	0.0215
2.5	0.0290	0.055	0.034	
3.0	0.037	0.057	0.031	
		$\sigma(D)\ \sqrt{2a}/\sqrt{D}$		
0.5	0.160	0.41	0.35	0.265
1.0	0.120	0.38	0.295	0.225
1.5	0.120	0.35	0.265	0.192
2.0	0.135	0.32	0.232	0.145
2.5	0.158	0.30	0.195	
3.0	0.190	0.28	0.150	
		Grain area $(\mu m)^2$		
0.5	0.0295	0.194	0.141	0.081
1.0	0.0166	0.166	0.100	0.058
1.5	0.0166	0.141	0.081	0.042
2.0	0.0210	0.118	0.062	0.0242
2.5	0.0287	0.104	0.044	
3.0	0.042	0.090	0.0260	

Table 11. Curve derived granularity values (HRP) -- HRP developer, 6.25 μm aperture.

Density	Exposing energy 20 KEV	15 KEV	10 KEV
	$\sigma(D)$		
0.5	-	0.032	0.0265
1.0	0.051	0.037	0.031
1.5	0.060	0.039	0.029
2.0	0.067	(0.042)	
2.5	0.070		
3.0	0.070		
	$\sigma(D)\ \sqrt{2a}/\sqrt{D}$		
0.5	0.48	0.39	0.32
1.0	0.43	0.34	0.25
1.5	(0.41)	0.31	(0.22)
2.0	(0.39)	0.27	
2.5	(0.37)	0.17	
3.0			
	Grain area $(\mu m)^2$		
0.5	0.265	0.175	0.118
1.0	0.213	0.133	0.072
1.5	(0.194)	0.111	(0.056)
2.0	(0.175)	0.084	
2.5	(0.158)	0.033	
3.0			

Bracketed values represent curve extrapolation.

where $\underline{M}$ is the number of electrons in the area used to measure $\sigma(\underline{D})$ and $\underline{\phi}$ is the number of grains produced per electron. This relationship was tested and the resultant value for $\underline{\phi}$ appears in Table 12. Since $\underline{\phi}$ is a function of electron range and this range increases with the squared acceleration potential, then $\underline{\phi}$ should increase with voltage in the sequence 1.0, 2.25, and 4.0. This appears to hold except for the 20 KEV exposures. This may be caused by an appreciable number of the higher energy electrons passing completely through the emulsion. Since the value for $\underline{\phi}$ was significantly less than unity, the exposure process was not a one hit process.

Table 12. Granularity compared to input noise -- Examination of the relation: $\sigma(D)/D = 1/\sqrt{N}(1+2/\phi)^{1/2}$, D-19 developer, 6.25 μm aperture.

KEV	$\frac{\sigma(D)}{D}\Big\|_{D=1}$	$1/\sqrt{N}$	$(1+2/\phi)^{1/2}$	ϕ	Ratio
10	0.024	0.00676	3.55	.17	1
15	0.032	0.0128	2.50	.38	2.2
20	0.043	0.0174	2.48	.39	2.3

Fréiser's (1959) relation between the electron produced $\sigma(\underline{D})_e$ and the light produced $\sigma(\underline{D})_p$ is:

$$\sigma^2(\underline{D})_e = (\underline{\phi} + 1)\sigma^2(\underline{D})_p. \qquad (36)$$

This relationship is presented in Table 13. At a density of one the values for $\underline{\phi}$ are ordered in the sequence 1.0, 2.3, 4.5, very near the expected sequence. Here, however, the values for $\underline{\phi}$ are greater than unity, contrary to the Valentine (1966) formula.

Table 13. Number of grains produced per electron -- Examination of the relation $\sigma^2(D)_{Electron} = (\phi+1)\sigma^2(D)_{Light}$.

Density	$(\sigma 20KV/\sigma n\nu)^2$	$(\sigma 15KV/\sigma n\nu)^2$	$(\sigma 10KV/\sigma n\nu)^2$
0.5	7.3	4.2	3.0
1.0	9.6	5.3	2.9
1.5	8.9	4.7	2.0
2.0	5.5	2.5	0.9
2.5	3.6	1.3	
3.0	2.4	0.7	

In order to examine either of these two relationships the parameter ϕ must be determined by grain counting which is beyond the scope of this investigation; however, the results predicted by the second formula appear more reasonable. The failure of the first formula may be due to the non-linearity of the density-exposure curve.

Curves correlating $\sigma(\underline{D})$ to the exposure in the measuring area and the $\underline{D}$ value for that exposure appear in Figure 29. The line $\sigma(\underline{D}) = 1/(\underline{E})^{1/2}$ represents the input shot noise for a density of 1.0, the line $\sigma(\underline{D}) = 3/(\underline{E})^{1/2}$ represents the input noise for a density of 3.0. The electron exposure $\sigma(\underline{D})$ curve shapes differ considerably from the input noise shapes showing a multiplication of input noise that varies with exposure. For this particular film the value of $\sigma(\underline{D})$, although related to the input noise, was more than a factor of two higher than the input, indicating that the DQE was less than 0.5.

Comparing the electron $\sigma(D)$ to the photon $\sigma(\underline{D})$ (Figure 30), the electron value is generally less than a factor of three higher. At higher densities the aggregate spacing should become closer; for this reason, the contribution to the total $\sigma(\underline{D})$ due to "clumping" should decrease and the $\sigma(\underline{D})$ due to the primary grain should become measurable. Therefore at this point the ration of $\sigma(\underline{D})$ for electrons and photons should approach one. In fact, at high densities, except for the 20 KEV exposures, the ratio

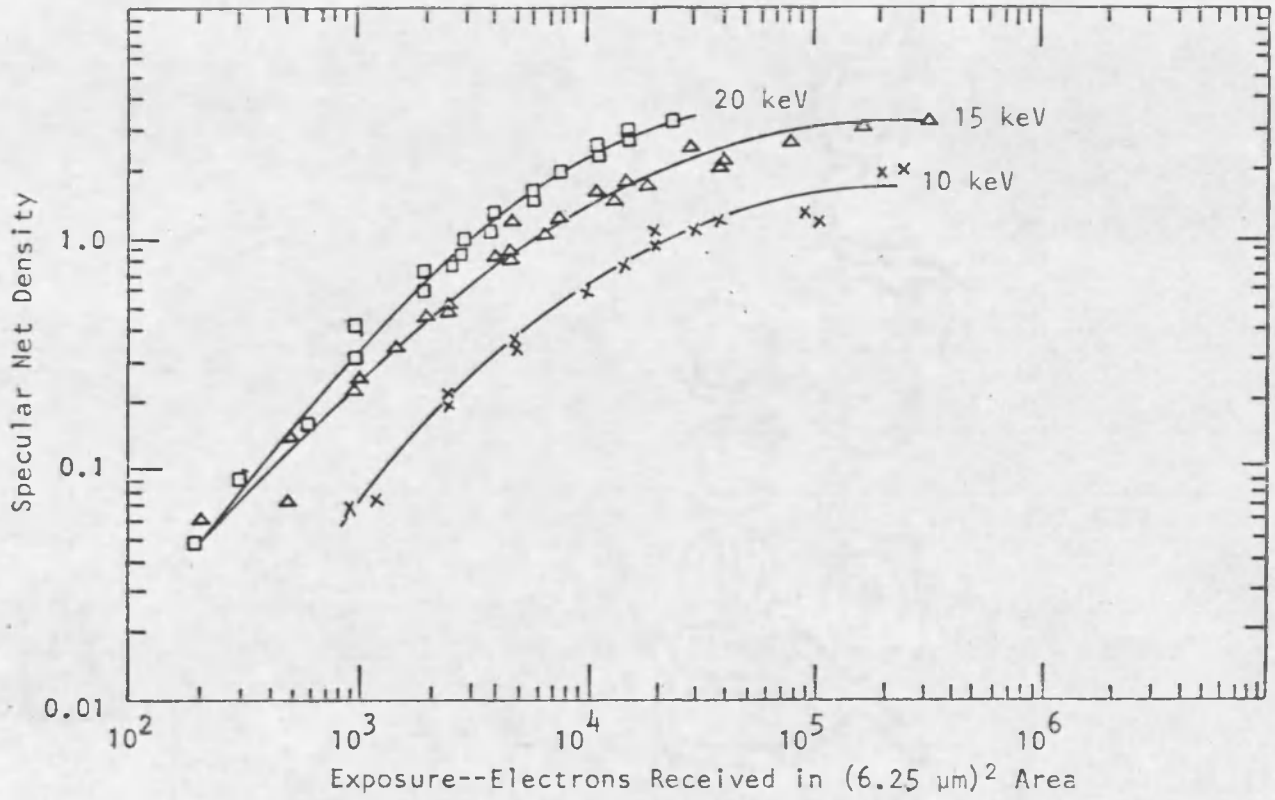

(a)

Figure 29. Variation of (a) D and (b) σ_D with exposure for D-19 with 6.25 μm aperture.

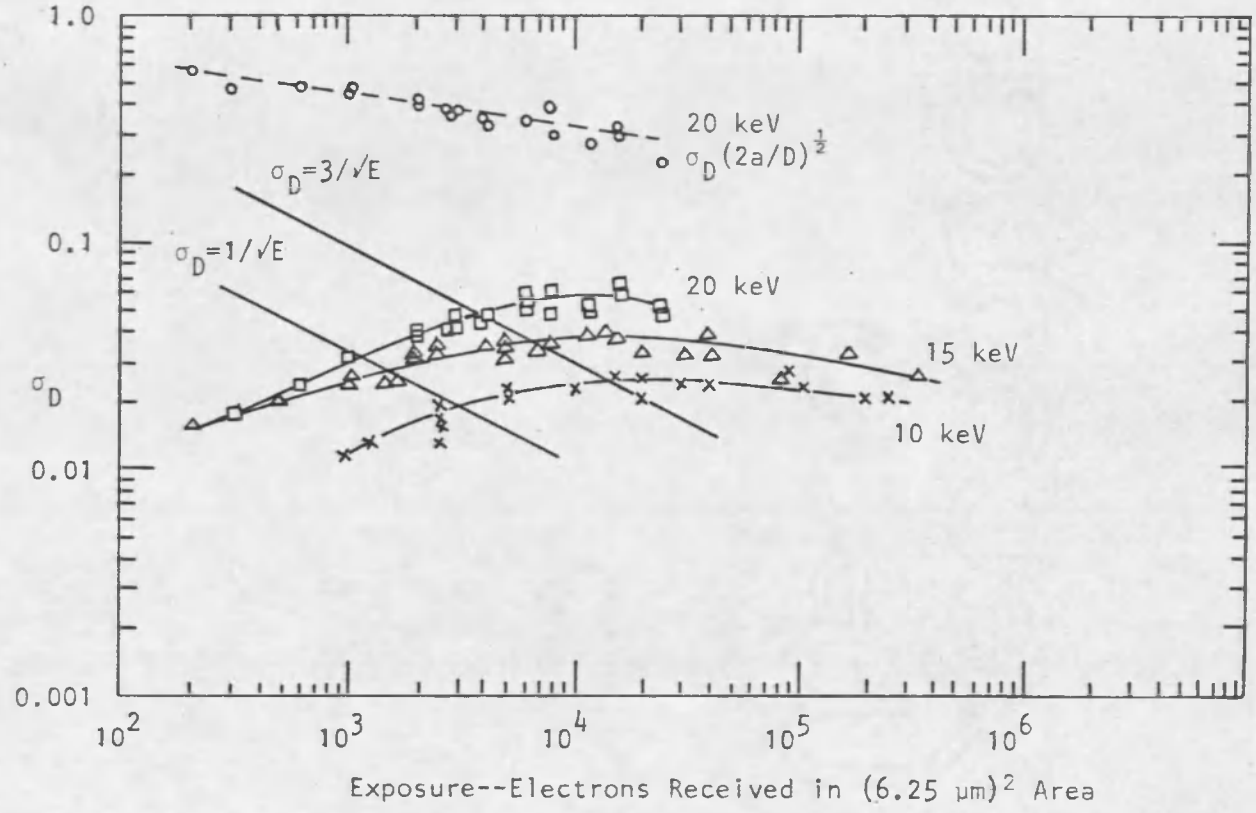

(b)

Figure 29.--Continued Variation of (a) D and (b) σ_D with exposure for D-19 with 6.25 μm aperture.

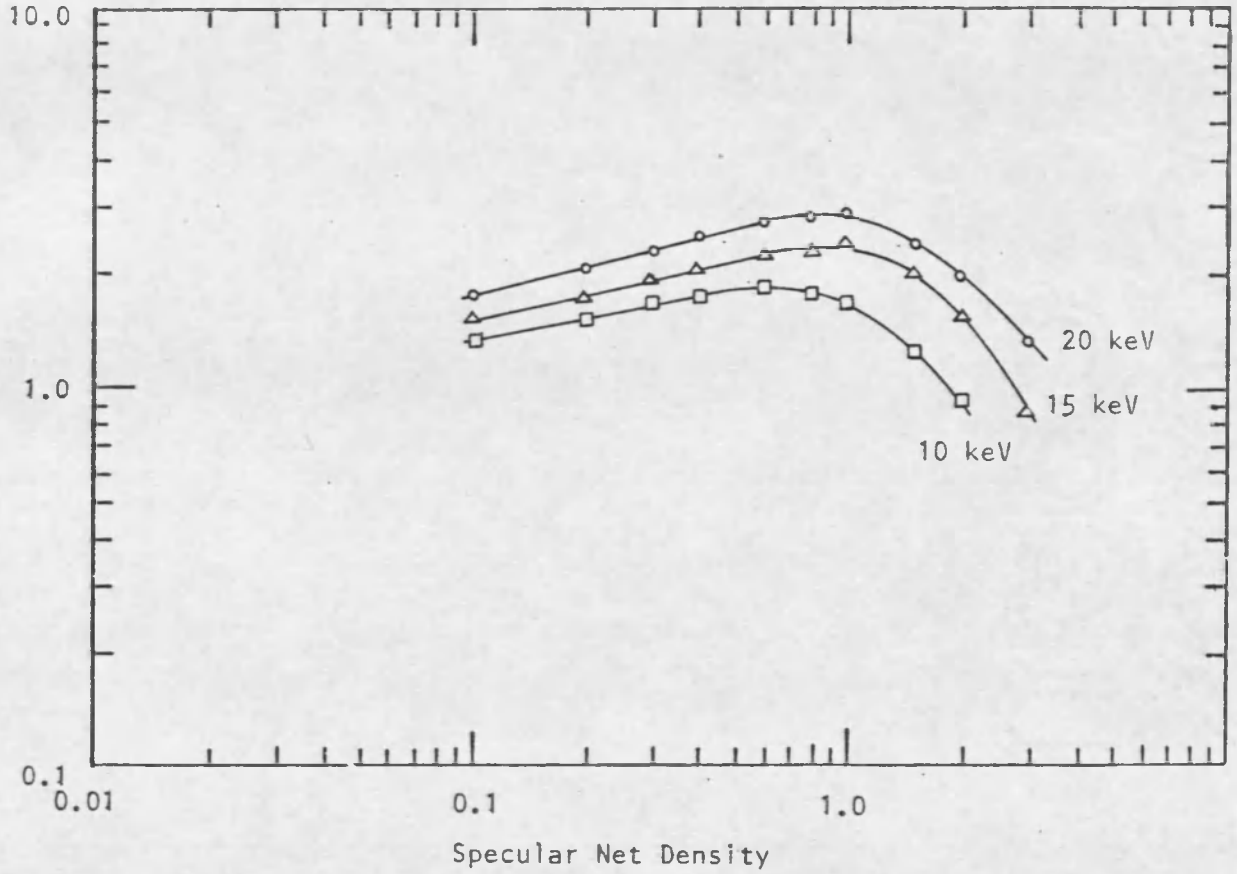

Figure 30. Comparison of electron and photon σ_D for (a) 1.57 μm aperture and (b) 6.25 μm aperture for D-19.

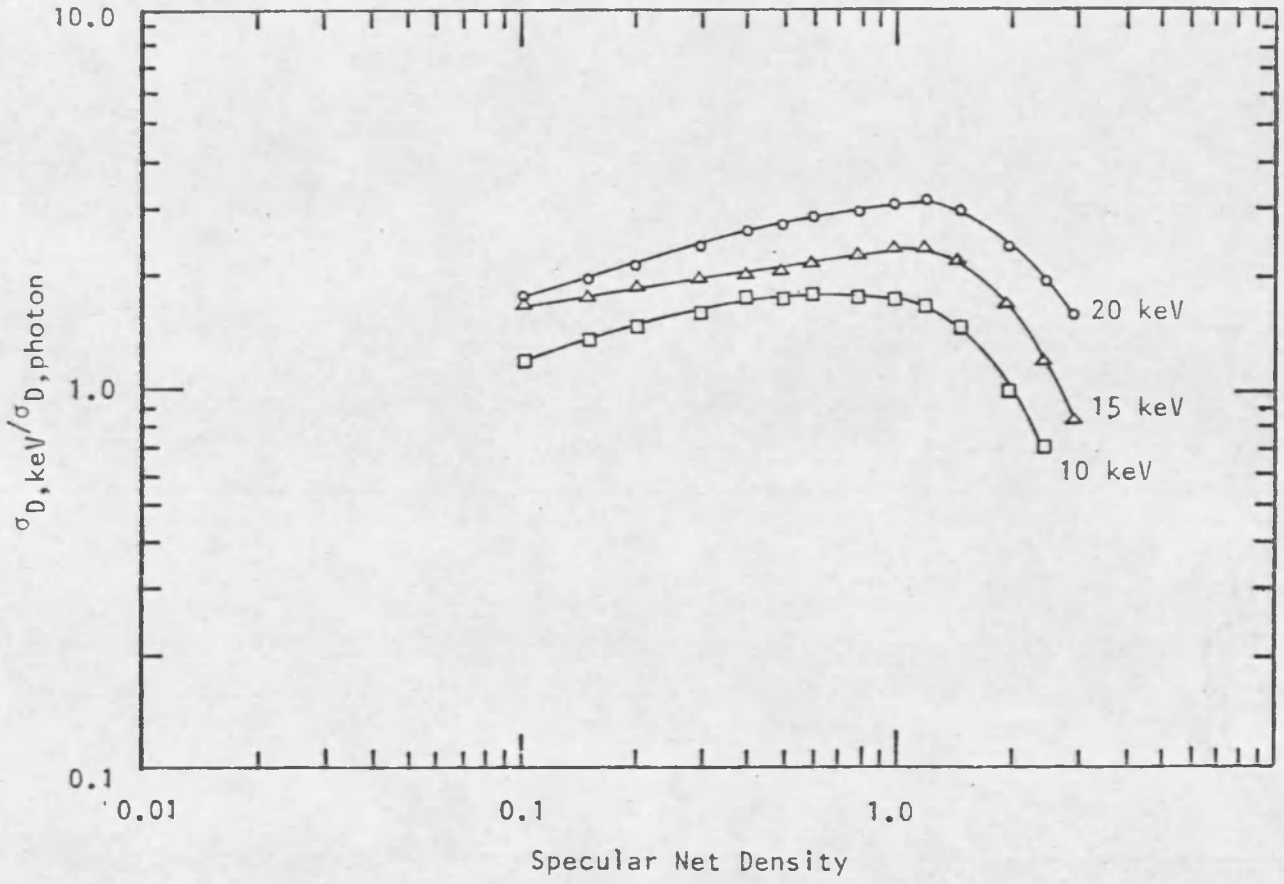

(b)

Figure 30.--Continued Comparison of electron and photon σ_D for (a) 1.57 μm aperture and (b) 6.25 μm aperture for D-19.

was less than one. However, only a single data point was statistically less than one after considering the experimental error.

RMS Granularity

The term RMS granularity as used by the Eastman Kodak Company generally means 1000 times the standard deviation of density when this deviation is measured with a circular aperture 48μm in diameter on a sample of unity density. Although the extrapolation from a square aperture 6.25μm on a side to a 48μm circle is possibly quite in error, the resultant extrapolated RMS granularity for the tested film was: 6.1, 4.9, and 4.0 for respective 20, 15, and 10 KEV electron exposures and 2.0 for photon exposures.

Summary

The macroscopic response curve for this material (SO-219) exposed to electrons had a lower slope than for photon exposures. Response linearity was not observed beyond a density of 0.75. Emulsion speed increased by a factor of four between 10 and 15 KEV electron exposures and by a factor of two between 15 and 20 KEV exposures.

Reciprocity failure was observed for 20 and 15 KEV exposures between intensity levels of 30 and 800 pico-amperes/cm^2. No failure was observed for 10 KEV exposures up to a density of 1.5 between intensity levels of 25 and 400 pa/cm^2.

Curves of $\sigma(\underline{D})$ plotted against $\underline{D}$ showed considerable differences between electron and photon exposures. Two square apertures were used to measure $\sigma(\underline{D})$, one 6.25μm on a side (measured to be 6.0 ± 0.25μm), and the other 1.57μm (measured 2.0 ± 0.25μm). Experimental error was estimated to be ±10% on $\sigma(\underline{D})$.

For photon exposures, $\sigma(\underline{D})$ increased slowly with $\underline{D}$ until a density of one where $\sigma(\underline{D})$ began to increase faster, an effect predicted by Bayer (1964). Below a density of one, the slopes of the Log $\sigma(\underline{D})$ - Log $\underline{D}$ curves were 0.086 and 0.18, respectively, for the large and small apertures; beyond this density the slopes were 1.0 and 0.81, again for the large and small apertures.

Electron exposures, however, differed from photon exposures in their Log $\sigma(\underline{D})$ - Log $\underline{D}$ curves. Initially Log $\sigma(\underline{D})$ increased with Log $\underline{D}$; then a maximum was reached, followed by a decrease. This maximum appeared to depend on the exposure energy level (acceleration voltage) and the maximum generally occurred near a density of 1.5. The slope of the curve, up to the maximum was between 0.37 and 0.30 for the small aperture and between 0.37 and 0.18 for the large.

Calculated grain areas were between 0.0166 and 0.042μm^2 for photon exposures and between 0.024 and 0.194μm^2 for electron exposures. Calculated grain areas increased with acceleration voltage and decreased monotonically with

density for the electron exposures. Photon exposures had calculated grain areas which decreased with an increase in density to a minimum near a density of one, then the sizes increased with density.

Valentine's (1966) relationship between $\sigma(\underline{D})$ and the exposure was not verified. The calculated ratio of the number of exposed grains per electron was lower than expected by the theory. Freiser's (1959) relationship between the electron $\sigma(\underline{D})$ and the photon $\sigma(\underline{D})$ was verified, although to verify each relationship an independent measurement of the grain/electron ratio would be required. Based on Freiser's equation and the observed $\sigma(\underline{D})$, the number of grains produced per electron was 8.3, 4.3, and 1.9, respectively, for 20, 15, and 10 KEV electron exposures. These values correlate well with the expected relative emulsion electron ranges of 4.0, 2.25, and 1.0.

The detective quantum efficiency was found to be about 0.3 instead of the expected 0.8-1.0. This is comparable to that reported by other investigators for slow, fine grained emulsions (Valentine, 1966; Valentine and Wrigley, 1964).

The RMS granularity referred to a 48μm diameter circular aperture and a density of one were 6.1, 4.9, 4.0, and 2.0, respectively, for 20, 15, and 10 KEV electrons and photon exposures. These values were calculated from the $\sigma(\underline{D})$ measured with a 6.25μm square aperture.

The number of distinguishable density levels ranged between 4 to 11 levels for electron exposures and was 15 levels for photon exposures. The lower values for electron exposures occurred with HRP developer which gave the most emulsion speed. The maximum value (11) occurred with 15 KEV electrons and with development in D-19 at an emulsion speed decrease of 25% compared to HRP developer.

APPENDIX

LIST OF SYMBOLS

Symbol	Definition
D-Log E	Density vs. Log Exposure
EBR	Electron Beam Recording
EVR	Electron Video Recording
MTF	Modulation Transfer Function
DQE	Detective Quantum Efficiency
DDL	Distinguishable Density Levels
A	Mean grain projected area
a	Cell area, spread function size, scanning aperture area
a'	Mean grain projected area
b	Constant
D	Density
D_{max}	Maximum density
d	Probability of a one electron exposure
e^-	Electron
E	Exposure, electrons or photons per unit area
F	Silver halicle/gelatine ratio
F(s)	Modulation transfer function (cycles per distance)
G,G'	Selwyn Granularity Coefficients
J_1	First order Bessel Function
k	Width

Symbol	Definition
KV	Kilo volts (potential)
KEV	Kilo electron volts (energy)
M	Average number of electrons in area a
N	Average number of grains in area a, noise
pa	Picoamperes (current)
Q	Opacity of a single grain
R	Electron range
r	Grain radius, number of absorbed quanta for developability
RMS	Root Mean Square
s	Spatial frequency, probability of a two electron exposure
S	Signal
S(x)	Spread function (distance)
T	Transmission
x	Spatial variable
Φ	Weiner (Power) spectrum
β	Granularity function
ϕ	Number of developed grains per electron
ε	Speed
σ	Standard deviation

LIST OF REFERENCES

Baker, R. F., Ramberg, E. G., and Hillier, J. "The Photographic Action of Electrons in the Range Between 40 and 212 Kilovolts," J. Appl. Phy. 13, 450 (1942).

Bayer, B. E. "Relation Between Granularity and Density for a Random-Dot Model," J. Opt. Soc. Am. 54, 1485 (1964).

Bendat, J. S., and Piersol, A. G. Measurement and Analysis of Random Data. New York: Wiley, 1966, p. 206.

Burge, R. E., and Garrard, D. F. "The Resolution of Photographic Emulsions for Electrons in the Energy Range 7-60 KEV," J. Sci. Inst. (J. Phys. E.), Series 2, 1, 715 (1968).

Burge, R. E., Garrard, D. F., and Browne, M. T. "The Response of Photographic Emulsions to Electrons in the Energy Range 7-60 KEV," J. Sci. Inst. (J. Phys. E.), Series 2, 1, 707 (1968).

Digby, N., Firth, K., and Hercock, R. J. "The Photographic Effect of Medium Energy Electrons," J. Phot. Sci. 1, 194 (1953).

Doerner, Edward C. "Wiener-Spectrum Analysis of Photographic Granularity," J. Opt. Soc. Am. 52, 669 (1962).

Dubbe, Richard F. "Television Film Recording Using Electron Exposure," J. SMPTE 75, 191 (1966).

Eastman Kodak Co. "Preliminary Technical Data--SO-159 Film," Eastman Kodak Data Sheet, Rochester, N. Y., 1968.

Eyer, James A. "The Influence of Emulsion Granularity on Quantitative Photographic Radiometry," Photo. Sci. Eng. 6, 71 (1962).

Freiser, H. "Messung des Schwankungsspektrums und der mittleren Schwarzung entwickelter photographischer Schichten," Mitt. Agfa 2, 249 (1958).

Freiser, H. "Noise Spectrum of Developed Photographic Layers Exposed by Light, X-Rays and Electrons," Phot. Sci. Eng. 3, 164 (1959).

Freiser, H., and Klein, E. "Die Eigenshaften photographischer Schichten bei Elektronenbestrahlung," Z. Angew. Phys. 10, 337 (1958) Translation Index T-2832 and TR-3686.

Freiser, H., Klein, E., and Zeitler, E. "Das Verhalten photographischer Schichten bei Electronenbestrahlung (II)," Z. Angew. Phys. 11, 190 (1959).

Hamilton, J. F., and Marchant, J. C. "Image Recording in Electron Microscopy," J. Opt. Sci. Am. 57, 232 (1967).

Haugh, E. F. "A Structural Theory for the Selwyn Granularity Coefficient," J. Phot. Sci. 11, 65 (1963).

Herbert, J. "Reading and Writing with Electron Beams," Electronics, p. 80, May 30, 1969.

Higgins, G. C., and Stultz, K. F. "Experimental Study of RMS Granularity as a Function of Scanning Spot Size," J. Opt. Soc. Am. 49, 925 (1959).

Jones, L. A., and Higgins, G. C. "Photographic Granularity and Graininess, II. The Effects of Variations in Instrumental and Analytical Techniques," J. Opt. Soc. Am. 36, 203 (1946).

Jones, R. C. "A Method of Describing and Measuring the Granularity of Photographic Materials," J. Opt. Soc. Am. 45, 799 (1955).

Kraus, W. "The Illumination of the Emulsion for Photographic Granularity Measurements," Phot. Sci. Eng. 12, 217 (1968).

Mannheim, L. A. "EVR: Movies and Microfilm on the TV Screen," Phot. Appl. in Sci. Tech. Med. 3, 16 (July, 1969).

Marathay, A. S., and Skinner, T. J. "Multilevel-Grain Model for Light Recording Media," J. Opt. Soc. Am. 59, 455 (1969).

Mees, C. E. K., and James, T. H. The Theory of the Photographic Process. 3rd Ed. New York: Macmillan, 1966.

Morimoto, H., Mori, N., and Sobue, Y. "Photographic Action of Electron (II), Analysis of Granularity," J. Soc. Sci. Phot. Jap. 25, 71 (1962) Translation Index T-4132.

Nitka, H. F. "Sensitivity and Detail Rendition in the Recording of Light Images and Electron Beams," Phot. Sci. Eng. 7, 188 (1963).

Reed, E. W. "An Electron Beam Television Recorder," J. SMPTE 75, 195 (1966).

Rickmers, A. D., and Todd, H. N. Statistics, an Introduction. New York: McGraw-Hill, 1967, p. 147.

Selwyn, E. W. H. "A Theory of Graininess," Phot. J. 75, 571 (1935).

Stultz, K. F., and Zweig, H. J. "Relation Between Graininess and Granularity for Black-and-White Samples with Nonuniform Granularity Spectra," J. Opt. Soc. Am. 49, 693 (1959).

Tajima, M. "Characteristics of Photographic Materials Exposed by Electron Beam (V), Physical Properties of Developed Images," J. Soc. Sci. Phot. Jap. 21, 121 (1958).

Takagi, A., Kitamura, N., and Morimoto, S. "Density vs. Exposure Curves of a Photographic Emulsion for 20-200 KV Electrons," J. Phys. Soc. Jap. 16, 792 (1961).

Tarnowski, A., and Evans, C. "Photographic Data Recording by Direct Exposure with Electrons," J. SMPTE 71, 765 (1962).

Thornley, R. F. M., Brown, A. V., and Speth, A. J. "Electron Beam Recording of Digital Information," IEEE Trans. on Elec. Comp. February, 1964, p. 36.

Valentine, R. C. "Characteristics of Emulsions for Electron Microscopy" in Quantitative Electron Microscopy, ed. G. F. Bahr and E. H. Zeitler. Baltimore: Williams and Wilkins, 1965.

Valentine, R. C. "Response of Photographic Emulsions to Electrons" in Advances in Optical and Electron Microscopy, Vol. 1. New York: Academic Press, 1966, p. 180.

Valentine, R. C., and Wrigley, N. G. "Graininess in the Photographic Recording of Electron Microscope Images," Nature 203, 713 (1964).

Van Horn, M. H. "The Use of Film in X-Ray Diffraction Studies," Rev. Sci. Inst. 22, 809 (1951).

Vernier, P. J. "Conditions for Linearity Between Density and Exposure for Photographic Plates," J. Opt. Soc. Am. 59, 444 (1969).

Webb, J. H. "Number of Quanta Required to Form the Photographic Latent Image as Determined from Mathematical Analysis of the H and D Curve," J. Opt. Soc. Am. 29, 309 (1939).

Zeitler, E. H., and Hayes, J. R. "Electrography" in Quantitative Electron Microscopy, ed. G. F. Bahr and E. H. Zeitler. Baltimore: Williams and Wilkins, 1965, p. 586.

Zweig, H. J. "Autocorrelation and Granularity. Part II. Results on Flashed Black-and-White Emulsions," J. Opt. Soc. Am. 46, 812 (1956).

3M Company. "EBR TV Recording System," advertisement J. SMPTE 77, 1237 (1968).

3M Company. "Series F Electron Beam Recording System," 3M Co. Information Manual, 1969.